duced into T cells. Here, we successfully transferred the cDNA library to a lentivirus vector and found that CD14 can confer resistance to HIV-induced cell death in the transduced cells. This observation suggests that the transferred libraries can still be applied for a functional screening system. Because the vector has also been used to transduce genes into nondividing cells such as neurons (11, 12), muscles (7), and hematopoietic stem cells (4), our lentivirus-based system can be applied to expression cloning systems that use such cells.

However, there is a need to improve our library transfer system. Some degree of loss in library complexity was noted. In our experiment, some of the cDNAs, especially long cDNA fragments, appeared to be lost during two steps: PCR amplification and lentivirus vector production and/or infection. This problem would be solved when the long cDNA fragments are enriched before the BP reaction and a genetic library is directly generated on a donor vector for the LR reaction. We think the latter strategy is useful because, if a library is constructed on a donor vector, the library can be transferred to various expression vector systems, which include not only the lentivirus vector but also other traditional vector systems, by only the LR reaction. As shown in Table 1, we did not observe the loss of library complexity during the LR reaction in our experiment. To overcome the loss of parts of the long cDNA fragments during production of lentivirus vector and/or infection, shorter parent lentiviral vector DNAs should be used in future experiments. In the present study, we used a GFP-expressing lentivirus vector DNA (CSII-EF-MCS-IRES-hrGFP). To obtain long cDNA inserts in the lentiviral vector, there is probably a need to delete some parts of the fragment within the vector DNA, such as IRES-hrGFP.

It was reported that the lentivirus (derived from HIV-1) vector-transduced T cells are less susceptible to wild-type HIV-1 infection than nontransduced T cells (3). The transcripts transduced by the vector appears to compete efficiently for encapsidation, resulting in inhibition of its infectivity, probably because *cis*-acting sequences in the lentivirus vector are responsive to the regulatory protein of wild-type HIV-1. However, the inhibitory effect was completely eliminated in a self-inactivating vector (3). Thus, we used a self-inactivating vector, and we could not actually find any differences in its HIV-1 replication ability between the transduced and nontransduced cells (data not shown).

In the present study, we used a cDNA library as a functional genetic element. In the future, we will be able to choose different genetic libraries, such as ribozyme (8) and peptide libraries (23, 25). The ribozyme library can be efficiently expressed under the control of an RNA polymerase III-dependent promoter (8). When constructing a lentivirus vector containing such a library, the Gateway-based transfer system will be useful. Moreover, since the length of such a library is more homogeneous and shorter than a conventional cDNA library, the lentivirus vector system will be able to more potently deliver a ribozyme library than a cDNA library.

CD14 is known as a coreceptor molecule for lipopolysaccharide (LPS) (24) and is expressed on the surface of myeloid cells via a glycosylphosphatidyl inositol tail. LPS binds to a serum protein, LPS-binding protein (15), and associates with CD14. Subsequently, LPS stimulates Toll-like receptor 4 (13) and activates signaling pathways, mainly the nuclear factor-κB (NF-κB) pathway. HIV-1 also preferentially infects macrophages that express CD14. It is known that macrophages are one of the major target cells for HIV infection, and they behave as cellular reservoirs of virions in HIV-infected patients, probably because the cells are relatively resistant to HIV-induced CPE (5). Although the mechanisms of the low susceptibility of macrophages to HIV-1-induced cell death are poorly understood at present, some explanations may be brought up from the resistance of CD14-transduced cells to HIV-1-induced cell death. One explanation is that overexpression of CD14 can trigger cell survival signals such as NF-κB or induce antiapoptotic genes. Another explanation is that CD14 can reduce the cytotoxicity of HIV-1 infection in T cells through a partial inhibition of HIV-1 replication. In fact, CD14 overexpression resulted in an inhibition of the entry step on HIV-1 replication, as shown in Fig. 5. A determination of the exact mechanisms of CD14 function in HIV-infected cells should enhance our understanding of the cellular events during HIV-induced cell death, which results in immune destruction in HIV-infected individuals.

In conclusion, application of the Gateway system to a genetic library transfer system will allow the use of the lentivirus vector system as a powerful tool for the study of functional genomics of mammalian cells.

ACKNOWLEDGMENTS

We thank I. Verma for providing several reagents used in our study.

This work was supported by a Grant-in-Aid for Scientific Research on Priority Areas from the Ministry of Education, Culture, Sports, Sciences, and Technology of Japan; by grants for Research on HIV-AIDS and Health Science from the Ministry of Health, Labor, and Welfare of Japan. Y. Koyanagi was also supported by a grant from the Naito Foundation.

REFERENCES

1. **Aruffo, A., and B. Seed.** 1987. Molecular cloning of a CD28 cDNA by a high-efficiency COS cell expression system. Proc. Natl. Acad. Sci. USA **84:** 8573–8577.
2. **Aruffo, A., and B. Seed.** 1987. Molecular cloning of two CD7 (T-cell leukemia antigen) cDNAs by a COS cell expression system. EMBO J. **6:**3313–3316.
3. **Bukovsky, A. A., J. P. Song, and L. Naldini.** 1999. Interaction of human immunodeficiency virus-derived vectors with wild-type virus in transduced cells. J. Virol. **73:**7087–7092.
4. **Case, S. S., M. A. Price, C. T. Jordan, X. J. Yu, L. Wang, G. Bauer, D. L. Haas, D. Xu, R. Stripecke, L. Naldini, D. B. Kohn, and G. M. Crooks.** 1999. Stable transduction of quiescent $CD34^+CD38^-$ human hematopoietic cells by HIV-1-based lentiviral vectors. Proc. Natl. Acad. Sci. USA **96:**2988–2993.
5. **Gartner, S., P. Markovits, D. M. Markovitz, M. H. Kaplan, R. C. Gallo, and M. Popovic.** 1986. The role of mononuclear phagocytes in HTLV-III/LAV infection. Science **233:**215–219.
6. **Hachiya, A., S. Aizawa-Matsuoka, M. Tanaka, Y. Takahashi, S. Ida, H. Gatanaga, Y. Hirabayashi, A. Kojima, M. Tatsumi, and S. Oka.** 2001. Rapid and simple phenotypic assay for drug susceptibility of human immunodeficiency virus type 1 using CCR5-expressing HeLa/$CD4^+$ cell clone 1–10 (MAGIC-5). Antimicrob. Agents Chemother. **45:**495–501.
7. **Kafri, T., U. Blomer, D. A. Peterson, F. H. Gage, and I. M. Verma.** 1997. Sustained expression of genes delivered directly into liver and muscle by lentiviral vectors. Nat. Genet. **17:**314–317.
8. **Ko, M. S. H.** 2001. Embryogenomics: developmental biology meets genomics. Trends Biotechnol. **19:**511–518.
9. **Kuwata, H., Y. Watanabe, H. Miyoshi, M. Yamamoto, T. Kaisho, K. Takeda, and S. Akira.** 2003. IL-10-inducible Bcl-3 negatively regulates LPS-induced TNF-α production in macrophages. Blood **102:**4123–4129.
10. **Miyoshi, H., K. A. Smith, D. E. Mosier, I. M. Verma, and B. E. Torbett.** 1999. Transduction of human $CD34^+$ cells that mediate long-term engraftment of NOD/SCID mice by HIV vectors. Science **283:**682–686.
11. **Naldini, L., U. Blomer, F. H. Gage, D. Trono, and I. M. Verma.** 1996. Efficient transfer, integration, and sustained long-term expression of the transgene in adult rat brains injected with a lentiviral vector. Proc. Natl. Acad. Sci. USA **93:**11382–11388.

12. **Naldini, L., U. Blomer, P. Gallay, D. Ory, R. Mulligan, F. H. Gage, I. M. Verma, and D. Trono.** 1996. In vivo gene delivery and stable transduction of nondividing cells by a lentiviral vector. Science **272**:263–267.
13. **Poltorak, A., X. He, I. Smirnova, M.-Y. Liu, C. V. Huffel, X. Du, D. Birdwell, E. Alejos, M. Silva, C. Galanos, M. Freudenberg, P. Ricciardi-Castagnoli, B. Layton, and B. Beutler.** 1998. Defective LPS signaling in C3H/HeJ and C57BL/10ScCr mice: mutations in Tlr4 gene. Science **282**:2085–2088.
14. **Reboul, J., P. Vaglio, N. Tzellas, N. Thierry-Mieg, T. Moore, C. Jackson, T. Shin-i, Y. Kohara, D. Thierry-Mieg, J. Thierry-Mieg, H. Lee, J. Hitti, L. Doucette-Stamm, J. L. Hartley, G. F. Temple, M. A. Brasch, J. Vandenhaute, P. E. Lamesch, D. E. Hill, and M. Vidal.** 2001. Open-reading-frame sequence tags (OSTs) support the existence of at least 17,300 genes in C. elegans. Nat. Genet. **27**:332–336.
15. **Schumann, R. R., S. R. Leong, G. W. Flaggs, P. W. Gray, S. D. Wright, J. C. Mathison, P. S. Tobias, and R. J. Ulevitch.** 1990. Structure and function of lipopolysaccharide binding protein. Science **249**:1429–1431.
16. **Seed, B.** 1995. Developments in expression cloning. Curr. Opin. Biotechnol. **6**:567–573.
17. **Seed, B., and A. Aruffo.** 1987. Molecular cloning of the CD2 antigen, the T-cell erythrocyte receptor, by a rapid immunoselection procedure. Proc. Natl. Acad. Sci. USA **84**:3365–3369.
18. **Shevchenko, Y., G. G. Bouffard, Y. S. Butterfield, R. W. Blakesley, J. L. Hartley, A. C. Young, M. A. Marra, S. J. Jones, J. W. Touchman, and E. D. Green.** 2002. Systematic sequencing of cDNA clones using the transposon Tn5. Nucleic Acids Res. **30**:2469–2477.
19. **Simpson, J. C., V. E. Neubrand, S. Wiemann, and R. Pepperkok.** 2001. Illuminating the human genome. Histochem. Cell Biol. **115**:23–29.
20. **Suzuki, Y., N. Misawa, C. Sato, H. Ebina, T. Masuda, N. Yamamoto, and Y. Koyanagi.** 2003. Quantitative analysis of human immunodeficiency virus type 1 DNA dynamics by real-time PCR: integration efficiency in stimulated and unstimulated peripheral blood mononuclear cells. Virus Genes **27**:177–188.
21. **van Maanen, M., J. K. Tidwell, L. A. Donehower, and R. E. Sutton.** 2003. Development of an HIV-based cDNA expression cloning system. Mol. Ther. **8**:167–173.
22. **Walhout, A. J. N. M., R. Sordella, X. Lu, J. L. Hartley, G. F. Temple, M. A. Brasch, N. Thierry-Mieg, and M. Vidal.** 2000. Protein interaction mapping in C. elegans using proteins involved in vulval development. Science **287**:116–122.
23. **Welch, P. J., E. G. Marcusson, Q.-X. Li, C. Beger, M. Kruger, C. Zhou, M. Leavitt, F. Wong-Staal, and J. R. Barber.** 2000. Identification and validation of a gene involved in anchorage-independent cell growth control using a library of randomized hairpin ribozymes. Genomics **66**:274–283.
24. **Wright, S. D., R. A. Ramos, P. S. Tobias, R. J. Ulevitch, and J. C. Mathison.** 1990. CD14, a receptor for complexes of lipopolysaccharide (LPS) and LPS binding protein. Science **249**:1431–1433.
25. **Xu, X., C. Leo, Y. Jang, E. Chan, D. Padilla, B. C. Huang, T. Lin, T. Gururaja, Y. Hitoshi, J. B. Lorens, D. C. Anderson, B. Sikic, Y. Luo, D. G. Payan, and G. P. Nolan.** 2001. Dominant effector genetics in mammalian cells. Nat. Genet. **27**:23–29.

European Journal of Neuroscience, Vol. 20, pp. 2499–2508, 2004

Intrinsic and spontaneous neurogenesis in the postnatal slice culture of rat hippocampus

Maki Kamada,[1] Ren-Yong Li,[1] Mika Hashimoto,[2] Masaaki Kakuda,[1,2] Hiroshi Okada,[3] Yoshio Koyanagi,[4] Toru Ishizuka[1,2] and Hiromu Yawo[1,2]
[1]CREST, JST, Kawaguchi 332–0012, Japan
[2]Department of Developmental Biology and Neurosciences, Tohoku University Graduate School of Life Sciences, 2–1 Seiryo-machi, Aoba-ku, Sendai 980–8575, Japan
[3]Department of Virology, Tohoku University Graduate School of Medicine, Sendai 980–8575, Japan
[4]Laboratory of Viral Pathogenesis, Institute for Virus Research, Kyoto University, Kyoto 606–8507, Japan

Keywords: adult neurogenesis, calbindin, dentate gyrus, enhanced green fluorescent protein, virus

Abstract

Organotypic slice culture preserves the morphological and physiological features of the hippocampus of live animals for a certain time. The hippocampus is one of exceptional regions where neurons are generated intrinsically and spontaneously throughout postnatal life. We investigated the possibility that neurons are generated continuously at the dentate granule cell layer (GCL) in slice culture of the rat hippocampus. Using 5-bromodeoxyuridine (BrdU) labelling and retrovirus vector transduction methods, the phenotypes of the newly generated cells were identified immunohistochemically. At 4 weeks after BrdU exposure, BrdU-labelled cells were found in the GCL and were immunoreactive with a neuronal marker, anti-NeuN. There were fibrils immunoreactive with anti-glial fibrillary acidic protein (GFAP), an astrocyte marker, in the layer covering the GCL and occasionally encapsulated BrdU-labelled nuclei. When the newly divided cells were marked with the enhanced green fluorescent protein (EGFP) using a retrovirus vector, these cells had proliferative abilities throughout the following 4-week cultivation period. Four weeks after the inoculation, the EGFP-expressing cells consisted of various phenotypes of both early and late stages of differentiation; some were NeuN-positive cells with appearances of neurons in the GCL and some were immunoreactive with anti-Tuj1, a marker of immature neurons. Some EGFP-expressing cells were immunoreactive with anti-GFAP or anti-nestin, a marker of neural progenitors. The present study suggests that slice cultures intrinsically retain spontaneous neurogenic abilities for their cultivation period. The combination of slice culture and retrovirus transduction methods enable the newly divided cells to be followed up for a long period.

Introduction

In the mammalian central nervous system, the hippocampus is one of regions where new neurons are generated intrinsically and spontaneously throughout the postnatal life of animals (Altman & Das, 1965; Cameron *et al.*, 1993; Gould *et al.*, 1999b; Kornack & Rakic, 1999) including humans (Eriksson *et al.*, 1998). These cells acquire neuron-like appearances with axons and dendrites (van Praag *et al.*, 2002), neuron-specific marker proteins such as NeuN and Tuj1 (Cameron *et al.*, 1993; Eriksson *et al.*, 1998; Kornack & Rakic, 1999; van Praag *et al.*, 2002) and neuron-like membrane properties such as action potentials and synaptic potentials (van Praag *et al.*, 2002) during the course of maturation. Moreover, these cells migrate to be integrated in the dentate granule cell layer (GCL), express calbindin D28K, a GCL cell marker protein (Kuhn *et al.*, 1996; Eriksson *et al.*, 1998) and project axons into the CA3 region (Hastings & Gould, 1999; Markakis & Gage, 1999). Neural stem cells derived from the adult hippocampus differentiate into neuron-like cells and form synaptic networks *in vitro* (Song *et al.*, 2002). These morphological and physiological features strongly suggest that the new neurons would be incorporated in the hippocampal local circuitry and that they would be involved in hippocampus-dependent memory formation (Shors *et al.*, 2001; Kempermann, 2002; van Praag *et al.*, 2002) and brain repair (Gould & Tanapat, 1997; Liu *et al.*, 1998; Kuhn *et al.*, 2001).

Organotypic cultures of hippocampal slices would provide an alternative model to hippocampus *in vivo* (Gähwiler *et al.*, 1997). As all types of neurons and glia are preserved with their specific morphologies and localizations in hippocampal slice cultures, the main network organization is very similar to that of living animals (Gähwiler, 1984; Zimmer & Gähwiler, 1984; Dailey *et al.*, 1994). However, a few rearrangements have been observed probably as a result of afferent deprivation (Robain *et al.*, 1994; Gutierrez & Heinemann, 1999). Neurons in slice culture maintained their physiological membrane properties and synaptic transmissions as well as several forms of short- and long-term plasticity (Gähwiler *et al.*, 1997). Therefore, slice cultures have been used widely in studies on physiology, pharmacology, morphology and the plasticity of the hippocampus.

It is plausible that hippocampal slice cultures have potencies to generate new neurons *in vitro* as suggested by the observations that neural progenitor-like cells are found in the slice culture (Miyaguchi, 1997) and transplanted ES cells differentiate into neurons (Benninger

Correspondence: Dr Hiromu Yawo, [2]Department of Developmental Biology and Neurosciences, as above.
E-mail: yawo@mail.tains.tohoku.ac.jp

Received 28 June 2004, revised 26 August 2004, accepted 30 August 2004

doi:10.1111/j.1460-9568.2004.03721.x

et al., 2003). The presence of neurogenic abilities has recently been reported in hippocampal slice cultures by 5-bromodeoxyuridine (BrdU) labelling methods (Raineteau *et al.*, 2004). In the present study the newly generated cells were also identified by retrovirus vector transduction methods. We found that hippocampal slice cultures retain endogenous neural progenitors in the dentate gyrus throughout the cultivation period and maintain *per se* the potential to differentiate spontaneously into neurons. We followed up the newly generated cells for a long period and found that some newly generated neurons are indeed incorporated into the normal architecture of GCL with the expression of one of the GCL cell markers, calbindin D28K.

Materials and methods

Slice culture

Hippocampal organotypic cultures were prepared according to the standard interface method (Stoppini *et al.*, 1991; Sakaguchi *et al.*, 1994). Hippocampal slices were prepared from postnatal day 7 Wistar rats (Nihon SLC Co., Japan). After decapitation, the brain was removed and transversely sliced at the hippocampus into a 350 μm thickness on a McIlwain tissue chopper (The Mickle Laboratory Engineering, UK). The isolated hippocampal slices were transferred onto a porous translucent membrane (Millicell-CM: PICM03050, Millipore, Billerica, MA, USA) and maintained in culture at 34 °C for several weeks in the interface between culture medium and a 5% CO_2 atmosphere. The culture medium in this experiment was a mixture of 50% commercial medium (OPTI-MEM, Invitrogen, Carlsbad, CA, USA), 25% heat inactivated horse serum (Invitrogen) and 25% Hank's balanced salt solution (Invitrogen) supplemented with D-glucose (5 g/L), penicillin (100 units/mL; Invitrogen) and streptomycin (100 μg/mL; Invitrogen), and was changed twice a week. Slices were also prepared from an adult female Wistar rat, as a control. The animal was deeply anaesthetized with diethyl ether then decapitated. The brain was removed and hippocampal slices (100 μm thickness) were prepared. All of the animal treatments used here were performed in accordance with the guidelines laid down by the Japan Neuroscience Society and NIH.

To label the immediately post-mitotic cells, slices at 13–14 days *in vitro* (DIV) were incubated for 3 days with culture medium containing 10 μM 5-bromodeoxyuridine (BrdU, Roche Diagnostics, Indianapolis, IN, USA) and then to normal medium. One to four weeks after BrdU treatment, the slices were fixed with 4% paraformaldehyde in 0.1 M sodium phosphate buffer for 1 h at 4 °C.

Retrovirus vector transduction

A murine leukaemia virus-based vector, SRαLEGFP (An *et al.*, 1999), was derived from SRαL*thy* (An *et al.*, 1997) by replacing the murine thy1.2 gene with enhanced green fluorescent protein (EGFP). Vector stocks were generated by calcium phosphate-mediated transfection of HEK 293T cells. HEK 293T cells were cultured in Dulbecco's modified Eagle medium with 10% calf serum, 100 units/mL penicillin and 100 μg/mL streptomycin in a 5% CO_2 incubator and transfected the following day with the envelope plasmid pMD.G (Zufferey *et al.*, 1997), the packaging plasmid pSVψ-E-murine leukaemia virus (Landau & Littman, 1992) and the transfer vector plasmid SRαLEGFP. At 24 h post-transfection, the medium was replaced with serum-free medium (OPTI-MEM; Invitrogen). At 48 h post-transfection, the virus-containing supernatant was collected, centrifuged and passed through a 0.45 μm filter. The virus vectors were further concentrated by centrifugation at 6000 *g* for 16 h at 4 °C. The pellet was resuspended in serum-free medium and kept in liquid nitrogen until use. Stocks of the vector were titrated by infecting NIH3T3 cells and analysing for EGFP expression by flow cytometry. The titre of vectors was 5×10^5 infectious units/mL.

Slices at 14 DIV were inoculated with the retrovirus vector encoding EGFP in the suprapyramidal region of the GCL. Then, 2–4 weeks later, the slices were fixed with 4% paraformaldehyde in 0.1 M sodium phosphate buffer for 1 h at 4 °C and used for immunohistochemical studies.

Zinc histofluorescence

The distribution of axons (mossy fibres; MFs) and their terminals in GCL neurons was investigated using a membrane-permeable zinc-sensitive fluorescent indicator, *N*-(6-methoxy-8-quinolyl)-*p*-toluenesulphonamide (TSQ, Molecular Probes, Eugene, OR, USA). TSQ (5 mg) was dissolved in 333 μL dimethyl sulphoxide (DMSO) containing 20% pluronic acid (Dojindo Laboratories, Kumamoto, Japan) and stored at 4 °C. A TSQ solution (1 : 250) was freshly prepared by adding Ca^{2+}-free Tyrode's solution, which reduced the release probability and thereby prevented translocation of the zinc from presynaptic terminals. The vital or freshly frozen slices at 2–6 weeks *in vitro* (WIV) were immersed in the TSQ solution for 30 min at 34 °C and briefly rinsed in Tyrode's solution containing EDTA disodium-calcium salt (Ca-EDTA, 10 mM) to chelate extracellular free zinc (Varea *et al.*, 2001). The slices were finally viewed by using a conventional epifluorescence microscope (BX51, Olympus, Tokyo, Japan) equipped with a WU excitation/detection filter and recorded using a digital camera system (PDMC-II, Polaroid, Cambridge, MA, USA).

Immunohistochemistry

The slices were fixed with 4% paraformaldehyde in 0.1 M sodium phosphate buffer at 4 °C for 1 h, then washed in PBS. For BrdU detection, the slices were incubated in 2 N HCl at 37 °C for 1 h to denature DNA, neutralized twice with 0.1 M borate buffer (pH 8.5) for 30 min and washed twice in PBS. After peeling the slices off from the membrane, all the subsequent procedures were carried out on free-floating slices using a rotator. The slices were blocked in PBS with 5% normal goat serum and 0.3% Triton X-100 at 4 °C overnight and reacted with the following primary antibodies in phosphate-buffered saline (PBS) with 5% normal goat serum and 0.3% Triton X-100 at 4 °C for 24 h: mouse monoclonal anti-NeuN (1 : 1000; Chemicon, Temecula, CA, USA), mouse monoclonal anti-βIII tubulin (Tuj1; 1 : 1000; Promega, Madison, WI, USA), mouse monoclonal anti-MAP2 (1 : 1000; Sigma-Aldrich, St Louis, MO, USA), mouse monoclonal anti-nestin (1 : 1000; Chemicon), guinea pig polyclonal anti-GFAP (1 : 1000; Advanced Immunochemical, Long Beach, CA, USA), rabbit polyclonal anti-GFAP (1 : 1000; Promega), rat monoclonal anti-BrdU [Clone:BU1/75 (ICR1); 1 : 100; Oxford Biotechnology, UK] or rabbit polyclonal anti-EGFP produced by Tamamaki *et al.* (2000) (1 : 500; a generous gift from Dr Y. Yanagawa, Gunma University, Japan). The preparations were then washed three times in PBS with 0.1% Triton X-100 and incubated at room temperature for 5–6 h with fluorescent dye conjugated secondary antibodies (each, 1 : 200) from different species: Alexa Fluor 546-conjugated anti-mouse IgG; Alexa Fluor 488-conjugated anti-guinea pig IgG; Alexa Fluor 488-, 546- or 633-conjugated anti-rat IgG; and Oregon Green 488-conjugated anti-rabbit IgG (all purchased from Molecular Probes). To ensure that our labelling patterns were not the conse-

quence of a dye artifact, double or triple immunolabelling was performed sequentially. After washing three times in PBS with 0.1% Triton X-100, the slices were mounted with Permafluor (Immunotech, France). Each specimen was analysed three-dimensionally with a z-axis interval of 0.87–0.88 μm under a conventional confocal laser microscope (LSM510META, Zeiss, Thornwood, NY, USA) equipped with 40 × objectives unless otherwise noted. The images were corrected for brightness and contrast using conventional software (LSM Image Browser version 3.2, Zeiss and Photoshop version 6.0, Adobe Systems Inc, San Jose, CA, USA).

Results

Cellular architecture of granule cell layer

Hippocampal slices prepared from postnatal rats were cultured for several weeks. The gross appearances of slices between 2 and 6 weeks of plating (Fig. 1, A2 and A3) were similar to those from the living intact animal (Fig. 1, A1) as noted in the previous studies (Stoppini *et al.*, 1991; Okada *et al.*, 1995). To further investigate the cellular architecture of the slice culture, neurons were identified by the expression of neuronal nuclei antigen (NeuN), which is expressed specifically in the nucleus of mature neuron with unknown functions (Mullen *et al.*, 1992). Similar to the living animal (Fig. 1, B1), GCL cells and pyramidal cell layer (PCL) cells of the CA1–4 region were preserved for as long as 6 WIV (Fig. 1, B2 and B3). The GCL was usually compact and clearly discriminated from the surrounding tissues in the suprapyramidal region whereas neurons formed a loose cluster and occasionally migrated out from the slices in the infrapyramidal region (e.g. Fig. 1, B2). To identify the GCL, all the following experiments were limited to the suprapyramidal region.

Next, we investigated whether the laminar arrangement of the slice culture assures optimal hippocampal networks. In the hippocampus *in vivo* the MF gives rise to fine collaterals with numerous small boutons in the hilus and traverses the apical dendritic shafts of CA3 pyramidal cells in a narrow band called the stratum lucidum (Henze *et al.*, 2000). Presynaptic boutons of the MF contain an exceptionally high concentration of zinc in the synaptic vesicles (Frederickson *et al.*, 2000). To identify the MF projection we applied a zinc sensitive fluorescent indicator, TSQ, which brightly

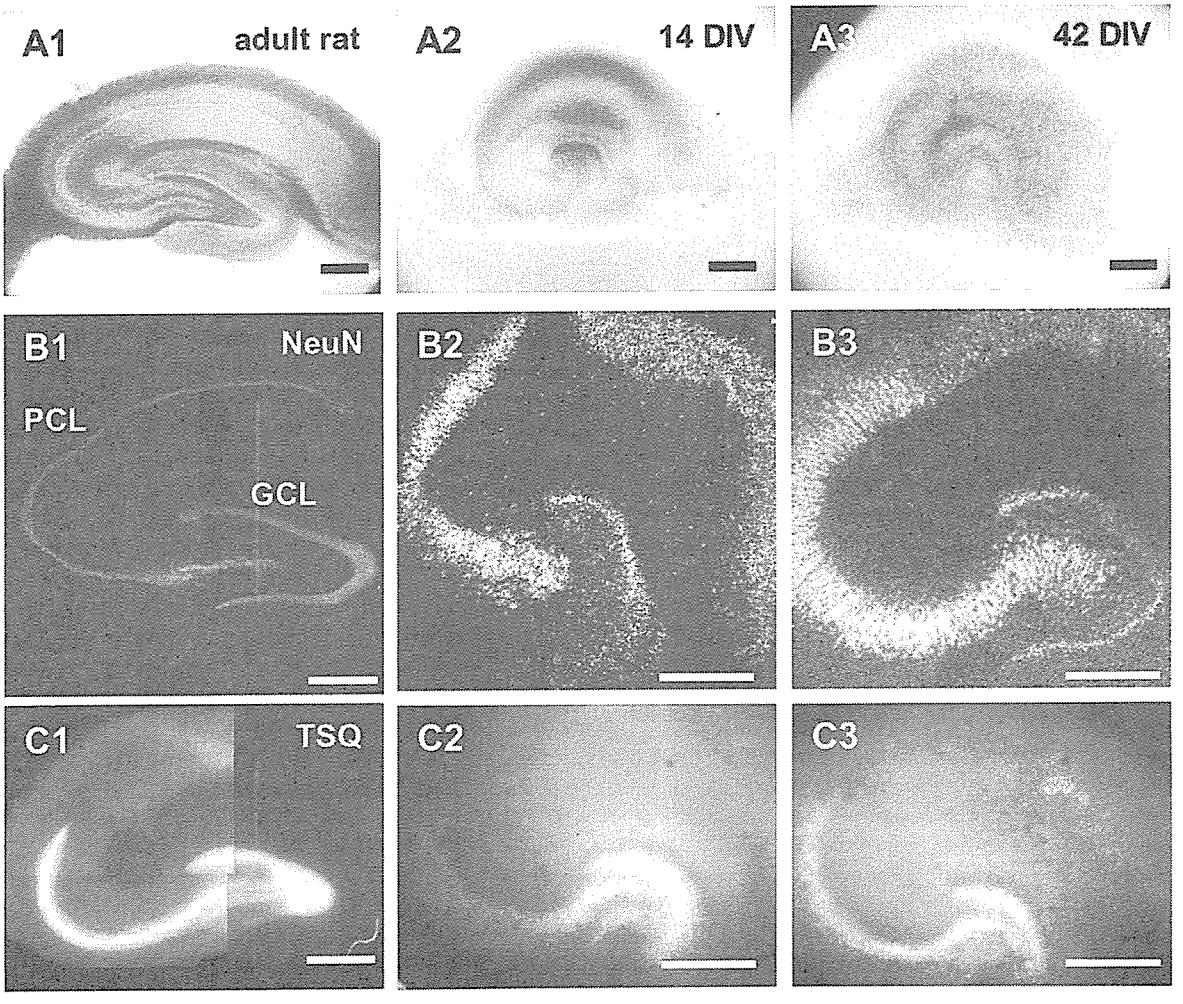

FIG. 1. The cellular architecture of rat hippocampal slice cultures. (A1–3) Plain views of hippocampal slice and its culture: the acute slice from an adult rat (A1), 14 DIV slice culture (A2) and 42 DIV slice culture (A3). (B1–3) The organizations of neuronal layers: the acute slice from adult rat (B1), 14 DIV slice culture (B2) and 42 DIV slice culture (B3). Neurons were immunolabelled with anti-NeuN, a neuron-specific marker. Note the presence of both the dentate granule cell layers (GCLs) and the CA1–4 pyramidal cell layers (PCLs). (C1–3) The laminar arrangements of mossy fibre (MF) projections: the acute slice from adult rat (C1), 14 DIV slice culture (C2) and 42 DIV slice culture (C3). The MFs and their terminals were visualized with a zinc-sensitive fluorescent indicator, *N*-(6-methoxy-8-quinolyl)-*p*-toluenesulphonamide (TSQ). The pattern of MF projections in the slice cultures is similar to that *in vivo*. Scale bars, 0.5 mm.

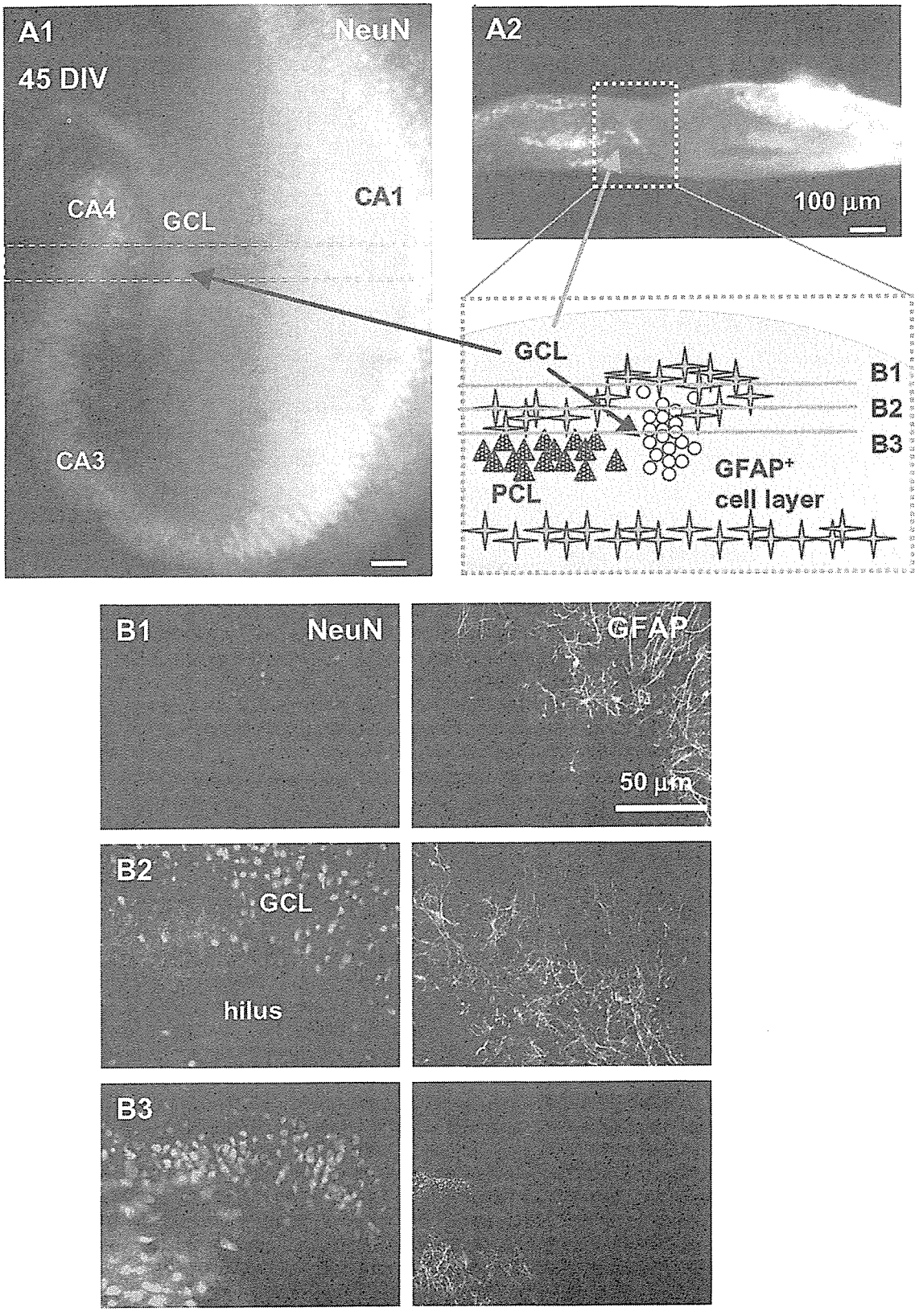

FIG. 2. Three-dimensional architecture of the dentate gyrus. (A1 and 2) The distribution of neurons in a 45 DIV slice culture: the horizontal (A1) and vertical (A2) appearances. Neurons were immunolabelled with anti-NeuN. The region between broken lines in A1 is viewed from the side in A2. The cartoon of cytoarchitecture corresponds to the square region in A2. The dotted lines, B1–3 correspond to the following panels B1–3, respectively. Neurons in the GCL and PCL are indicated by circles and triangles, respectively, and astrocytes by stars. The unidentified structure of slice culture is coloured in grey. (B1–3) The three-dimensional distribution of neurons and astrocytes in the dentate gyrus of a slice culture 6 μm above the layer of GCL (B1), the layer where GCL first appears (B2) and 6 μm below B2 (B3). The double immunofluorescent images of anti-NeuN (left), anti-GFAP (right) were obtained by using confocal microcopy.

labels the following regions (Fig. 1, C1): hilus of dentate gyrus; CA3 suprapyramidal and infrapyramidal layer. These brightly fluorescent regions were almost identical to those obtained with other metal-histochemical methods like Timm staining method (Frederickson *et al.*, 1987; Vogt *et al.*, 2000). Throughout the cultivation period TSQ brightly labelled these regions in some slices: 40.0% ($n = 25$) at 14 DIV (Fig. 1, C2); and 31.5% ($n = 108$) at 42 DIV (Fig. 1, C3). However, MF projections were obscure in others, probably through the massive reorganization of axonal trajectories or the ectopic projections in slice cultures (Robain *et al.*, 1994; Gutierrez & Heinemann, 1999). As the presence of robust MF projections is an indication of the preservation of efficient hippocampal architecture, all the following experiments were carried out after TSQ identification of MF projections.

Three-dimensional architecture of the dentate gyrus

Even when hippocampal slice cultures had preserved laminar structures for several weeks, the slices were flattened within the first week and maintained their thickness for subsequent weeks, as reported previously (Buchs *et al.*, 1993). To determine the position and thickness of the GCL in the slice culture, slices at 45 DIV were cut in a perpendicular plane to the Millicell-CM membrane along the CA1–4 axis, which had been previously fixed and immunolabelled for anti-NeuN (Fig. 2, A1). Slices had thinned to 179 ± 12 μm ($n = 11$; Fig. 2, A2) from the previous thickness of 350 μm. The PCL was stretched horizontally at CA1, as reported previously (Buchs *et al.*, 1993), whereas the GCL (thickness of tens of micrometres) was buried in the middle of the slice and was densely packed with neurons with small-sized nuclei.

To resolve the three-dimensional cytoarchitecture of the dentate gyrus, the culture slices at 45 DIV were immunolabelled with anti-NeuN and anti-glial fibrillary acidic protein (GFAP), specific antibodies to one of intermediate filament proteins and one of selective markers of astrocytes and radial glia (Ludwin *et al.*, 1976; Seri *et al.*, 2001), and inspected by using confocal laser scanning microscopy from the surface to the bottom (see Fig. 2 cartoon). There was a layer of GFAP-positive cells just above the GCL (Fig. 2, B1). In the layer containing the GCL, there was a dense cluster of NeuN-positive small nuclei, surrounded by GFAP-positive cells (Fig. 2, B2). In the deeper layer, NeuN-positive cells were found in the GCL as well as the PCL at CA4 (Fig. 2, B3). Although we did not determine the type of cells located under the neuronal somatic area, GFAP-positive processes sometimes tightly formed a thin layer in a vicinity of the Millicell-CM membrane.

Differentiation of endogenous progenitors in slice cultures

To investigate whether endogenous progenitors exist intrinsically and actually differentiate into neurons in the slice culture, we added BrdU, a thymidine analogue, to the culture medium. As BrdU is incorporated into nuclei during the S-phase, it should label the newly generated cells in slice cultures. The phenotype of BrdU-labelled cells was identified immunohistochemically using antibodies to neuronal or glial markers, under higher magnification. Usually, the suprapyramidal region of the GCL was set in the centre of the optical field, and the optical planes above and in the GCL were examined. In the case of slices at 45 DIV, triple immunofluorescent labelling (anti-BrdU, anti-NeuN and anti-GFAP) was carried out to identify the specific phenotypes of BrdU-labelled cells.

One week after BrdU treatment, many BrdU-labelled cells were found in and around the GCL, and occasionally appeared as pairs being opposed each other (Fig. 3, B1 and B3, arrowheads), but were coexpressed with neither NeuN (Fig. 3, A1–3) nor microtubule-associated protein 2 (MAP2; Fig. 3, B1–3), one of the cytoskeletal proteins expressed specifically in neuronal cell bodies and dendrites (Bernhardt & Matus, 1984). Many of these BrdU-labelled nuclei did not associate with GFAP-positive structures overlaying the GCL (Fig. 3, C1-3). However, under close inspection of three-dimensional structures, a few BrdU-labelled nuclei were encapsulated by the GFAP-positive fibres (asterisk). Some BrdU- and GFAP-positive cells had characteristic short processes (Fig. 3C, insets). These BrdU-labelled cells might also include non-neuronal and non-glial cells as microglia and fibroblasts although both cells are supposed to be few in the region around the GCL (Raineteau *et al.*, 2004).

Four weeks after treatment, confocal images revealed that some of the BrdU-labelled nuclei were coexpressed with NeuN in the GCL (Fig. 4, A1–3, arrowheads). These cells were not immunoreactive with anti-GFAP (Fig. 4, A4). The coexpression of BrdU and NeuN was examined three-dimensionally under higher magnification (Fig. 4B). In the layer overlaying the GCL, there were some BrdU-labelled nuclei surrounded by GFAP-positive processes (Fig. 4, C1–3, arrows). These cells were not immunolabelled by anti-NeuN (Fig. 4, C4).

Visualization of endogenous neurogenesis in living slices

The BrdU-labelling method has several disadvantages for the study of neurogenesis. Neurogenesis is only retrospectively identified in fixed tissues. Labelling with BrdU is not sufficient to prove that a given cell has divided because BrdU is a marker of DNA synthesis rather than of cell division (Rakic, 2002). BrdU-labelling alone does not reveal morphological characteristics of the newly generated cells as BrdU is incorporated into only their nuclei. Finally, the cellular and physiological features of living cells are difficult to investigate. To overcome these disadvantages, we marked endogenous progenitors in living slice cultures with EGFPs using retrovirus vectors, which were injected locally into the suprapyramidal region of the GCL. As the retroviruses infect only dividing cells and their genes are incorporated into the host's genomic DNA, newly divided cells and their descendants would specifically express EGFP.

From daily observations of the injected sites under fluorescent microscopy, the EGFP-expressing cells showed a tendency to increase in number between 1- and 2-weeks post-inoculation (Fig. 5, A1 and A2). The number of EGFP-expressing cells was followed up in six slices in which more than four EGFP-expressing cells were identified in the DGL 1 week after retrovirus vector inoculation and was even increased in the next 1–3 weeks (Fig. 5B). The relative number increased to 253 ± 58% (mean ± SEM; $n = 5$) in 1 week and to 296 ± 104% ($n = 4$) in 2 weeks. As our retrovirus vector is replication-incompetent, the EGFP-expressing cells proliferated as a result of mitosis. In the first 1–2-weeks post-inoculation, the typical EGFP-expressing cells were small with short processes (Fig. 5A), being reminiscent of the undifferentiated cells that had recently appeared. Indeed, three-dimensional analysis of confocal images revealed that 36 ± 4% (mean ± SEM; four slices, sum of double positive cells/total EGFP-expressing cells = 45/128) of these cells expressed nestin, one of intermediate filaments expressed specifically in neuroblasts and myoblasts (Lendahl *et al.*, 1990) and a putative neural precursor markers (see also Fig. S1 in Supplementary material). By contrast, the EGFP-expressing cells have neither neuronal appearances nor detectable NeuN immunoreactivities in these early

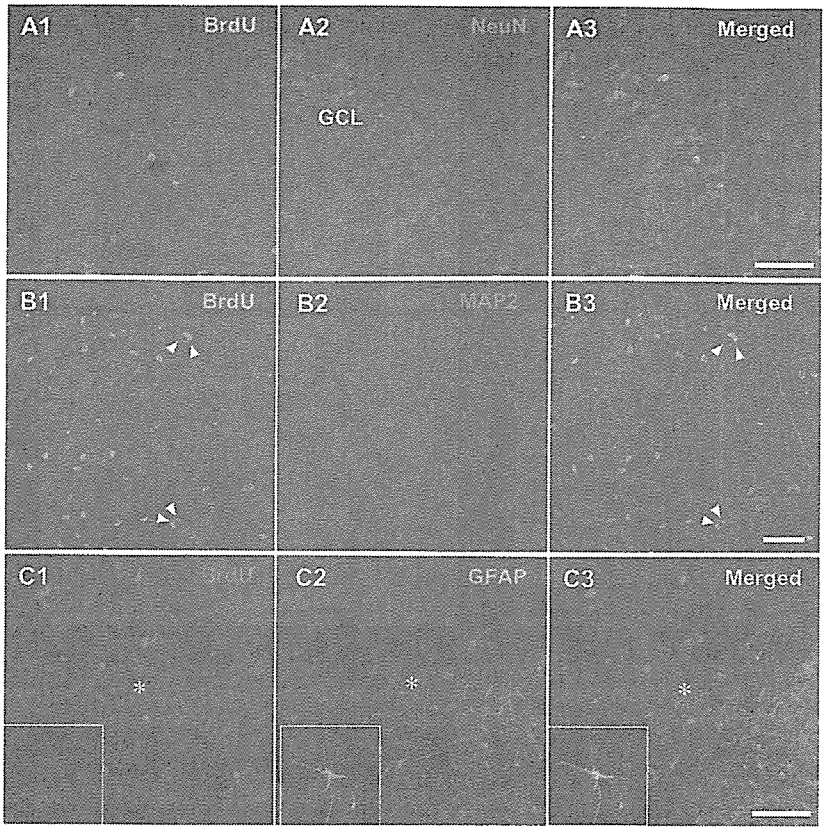
A1
BrdU
A2
NeuN
GCL
A3
Merged
B1
BrdU
B2
MAP2
B3
Merged
C1
BrdU
C2
GFAP
C3
Merged

FIG. 3.

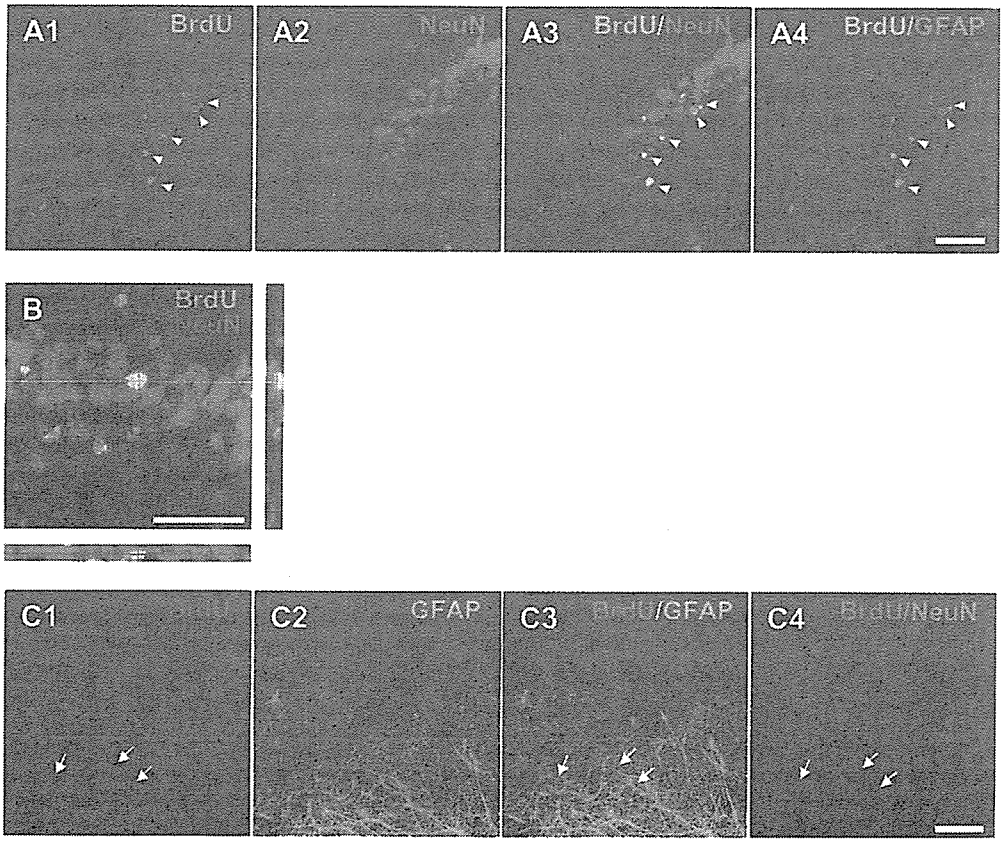
A1
BrdU
A2
NeuN
A3
BrdU/NeuN
A4
BrdU/GFAP
B
BrdU
C1
C2
GFAP
C3
C4
BrdU/NeuN

FIG. 4.

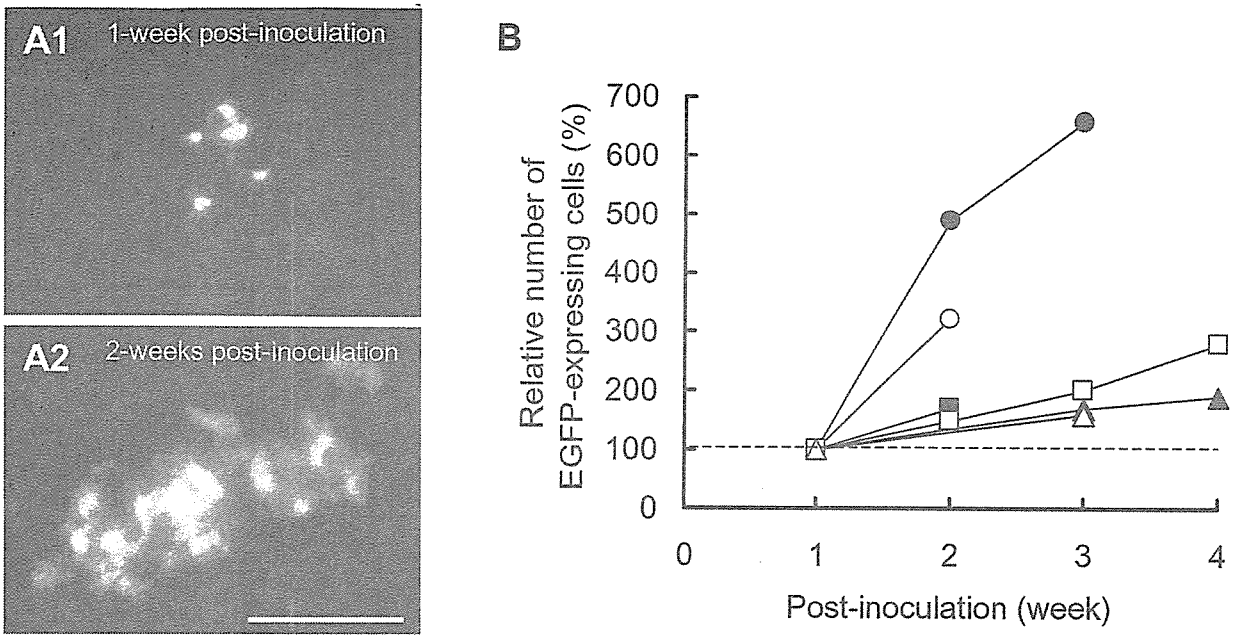

FIG. 5. Proliferation of enhanced green fluorescent protein (EGFP)-expressing cells after retrovirus vector inoculation. (A) The EGFP-expressing cells in the dentate gyrus at 1- (A1) and 2-weeks (A2) post-inoculation in the same place. Scale bar, 50 μm. (B) The number of EGFP-labelled cells in the dentate gyrus was counted, normalized to that seen at 1-week postinoculation and plotted against time. Each symbol represents an identical slice culture ($n = 6$).

postinoculation periods, indicating that our retrovirus vectors would not transfect mature neurons.

Some of the EGFP-expressing cells extended processes in the late WIV

Three-dimensional analysis of confocal images were investigated for phenotypes of EGFP-expressing cells 4 weeks after inoculation. Typical EGFP-expressing cells were seen in the GCL with several dendrite-like processes (Fig. 6A) and one elongated axon-like process (Fig. 6A, arrowheads) bearing putative synaptic boutons (Fig. 6A, arrow). The coexpression of EGFP and NeuN (Fig. 6B) was examined three-dimensionally under higher magnification (Fig. 6C). Some of these cells were immunoreactive to anti-NeuN and were incorporated in the normal architecture of GCL (Fig. 6A and B). Some EGFP-expressing cells represented early phenotypes of differentiation into neurons in the GCL with short processes and immunolabelled with antibodies to Tuj1 (Fig. 6D), one of the cytoskeletal proteins expressed specifically in immature neurons (Lee *et al.*, 1990). The detailed morphology of neuron-like EGFP-expressing cells also varied, as shown in Fig. 6A and B. Some dendrite-like processes extended to z-axis directions whereas others were horizontal. Some axon-like processes extended in the direction of CA3 pyramidal cells whereas in others it was the opposite. We tracked these axons for a considerable length but were unable to find the final destinations. To test if these EGFP-expressing cells have phenotypes of GCL neurons, the coexpression of EGFP and calbindin D28K, one of calcium binding proteins expressed specifically in some types of neurons including DGL cells (Baimbridge & Miller, 1982; Bousez-Dumesnil *et al.*, 1989) was examined three-dimensionally under a higher magnification (Fig. 6E). Indeed, there were the neuron-like EGFP-expressing cells immunoreactive to calbindin D28K in the DGL. These results are consistent with the notion that the slice cultures intrinsically retain a neurogenic potential qualitatively similar to the hippocampus in the living animal.

To investigate the occurrence of neuronal differentiation, retrovirus vectors were injected on the same day in the same place of the suprapyramidal region of the DGL of 14 DIV slice cultures derived from 10 littermates of either gender and prepared on the same day. Four weeks after inoculation, 14 slice cultures were selected for analysis of phenotypes because they had numbers (> 10) of EGFP-expressing cells. The immunoreactivity to anti-NeuN was investigated

FIG. 3. Phenotypes of newly generated cells in the dentate gyrus one week after incorporation of 5-bromodeoxyuridine (BrdU). (A1–3) The double immunofluorescent confocal images of GCL: anti-BrdU (A1, green), anti-NeuN (A2, red) and the merge (A3). (B1–3) The double immunofluorescent confocal images of GCL: anti-BrdU (B1, green), anti-MAP2 (B2, red) and the merge of both (B3). The double arrowheads indicate mitotic figures. (C1–3) The double immunofluorescent confocal images of the dentate gyrus: anti-BrdU (C1, red), anti-GFAP (C2, green) and the merge (C3). The asterisk indicates the BrdU-labelled GFAP-positive cell. Inset shows another BrdU-labelled GFAP-positive cell with processes clearly visible. Scale bars, 50 μm.

FIG. 4. Phenotypes of newly generated cells in the dentate gyrus four weeks after incorporation of BrdU. (A1–4) The triple immunofluorescent confocal images of GCL: anti-BrdU (A1, green), anti-NeuN (A2, red), the merge of both (A3) and the merge of anti-BrdU and anti-GFAP (blue) images (A4). The arrowheads indicate the newly generated neurons which are both BrdU-labelled and NeuN-positive. (B) Three-dimensional confocal micrograph showing a typical BrdU/NeuN-immunoreactive cell. The x–z and y–z images were accompanied. Note that BrdU distributes in the nucleus of the NeuN-positive cell in the DGL. (C1–4) Triple immunofluorescent confocal images of the layer overlaying GCL: anti-BrdU (C1, red), anti-GFAP (C2, green), the merge (C3) and the merge of anti-BrdU and anti-NeuN (blue) images (C4). The arrows indicate the BrdU-labelled GFAP-positive cell. Scale bars, 50 μm.

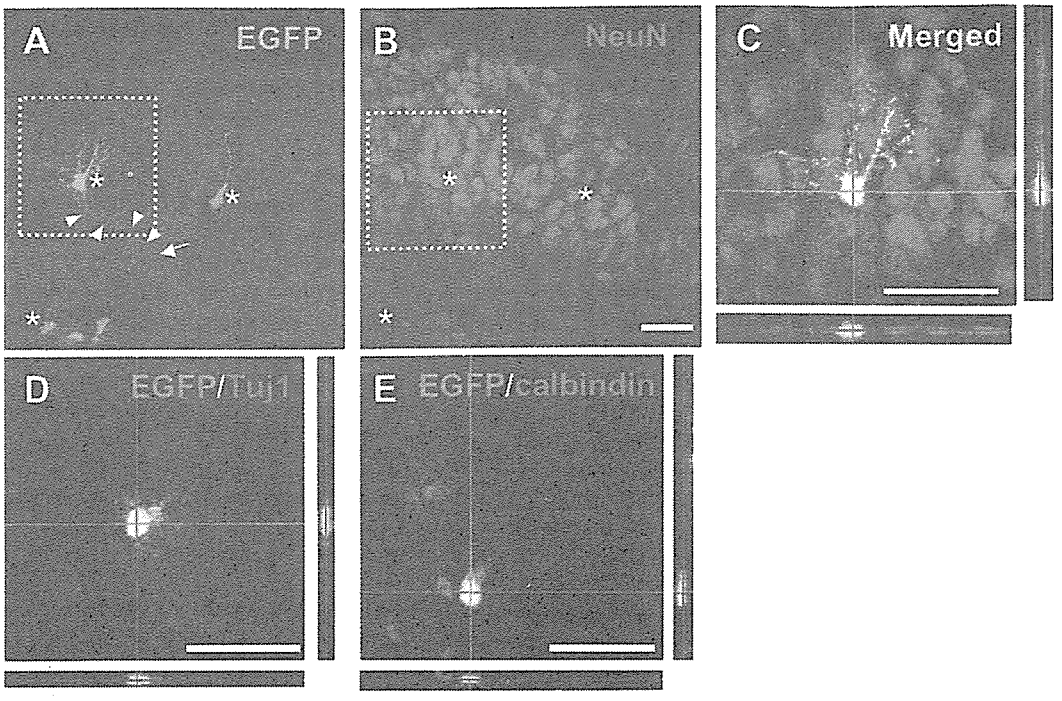

FIG. 6. Emergence of neuronal phenotypes in EGFP-expressing cells four weeks after retrovirus vector inoculation. (A and B) The double immunofluorescent confocal images of GCL: anti-EGFP (A, green), anti-NeuN (B, red). Typical EGFP-expressing NeuN-positive cells bear dendrite-like processes and an axon-like process (arrowheads) with a terminal bouton-like structure (arrow). EGFP-expressing cells that are immunoreactive with anti-NeuN are indicated by asterisks. (C) Three-dimensional analysis of a NeuN-positive EGFP-expressing cell. A rectangular region in A and B were merged and enlarged with x–z and y–z images. (D) Three-dimensional analysis of a double immunofluorescent confocal image of GCL: anti-EGFP (green) and anti-Tuj1 (red). The x–z and y–z images were accompanied. (E) Three-dimensional analysis of a double immunofluorescent confocal image of GCL: anti-EGFP (green); anti-calbindin D28K (red). The x–z and y–z images were accompanied. Scale bars, 50 μm.

in four slices. The NeuN-positive cells were found in the range of 10–40% of the EGFP-expressing cells. In total 23 of 91 EGFP-expressing cells were NeuN-positive (25%). The Tuj1-positive cells were in the range of 10–40% of the EGFP-expressing cells (four slices) and 23 of 94 EGFP-expressing cells in total (24%). Therefore, some but not all newly divided cells express neuronal phenotypes (see Fig. S1 in Supplementary material). In fact, in this series of experiments, the GFAP-positive cells were in the range of 10–40% of the EGFP-expressing cells (three slices) and 33 of 103 EGFP-expressing cells in total (32%). The nestin-positive cells were in the range of 10–40% of the EGFP-expressing cells (four slices) and 36 of 133 EGFP-expressing cells in total (27%).

Discussion

We made several observations reinforcing the previous study that postnatal hippocampal slice cultures preserve endogenous neuronal progenitor cells in the dentate gyrus, in which new neurons are spontaneously generated (Raineteau *et al.*, 2004). With BrdU used to label dividing cells, we found that some BrdU-labelled cells acquire phenotypes of mature neurons in the following four weeks. Using retrovirus vectors, we found that in 4 weeks some EGFP-expressing cells also acquire phenotypes of mature neurons extending dendrites and axon-like processes.

Differences between labelling methods

One of our new findings is that EGFP-expressing cells proliferated in the explanted hippocampus during the cultivation period between 1- and 4-week postinoculation (Fig. 5). This is in contrast to the observation that the number of BrdU-labelled cells has a tendency to decrease in days after early proliferation (Hayes & Nowakowski, 2002). Since BrdU is incorporated into DNA during mitosis, its density diminishes during the following cell divisions (Dayer *et al.*, 2003). Therefore, the descendents of highly proliferative cells would become negligible regarding BrdU immunoreactivity. Alternatively, the undifferentiated cells might be selected for survival before differentiation with massive cell death (Gould *et al.*, 1999a). Either way, it is generally accepted that BrdU preferentially labels the immediately post-mitotic cells during the period of drug exposure. By contrast, the retrovirus vector transduction reveals a different population of cells, the newly divided ones and their descendents.

Neurogensis in the slice culture system

In this study some BrdU-labelled cells in the GCL were also positive for NeuN, a marker of mature neurons (Fig. 4A and B). These observations are consistent with reports of *in vivo* preparations (Kuhn *et al.*, 1996; Eriksson *et al.*, 1998; Kornack & Rakic, 1999) and slice culture systems (Raineteau *et al.*, 2004), and imply that intrinsic neural progenitors are present in the hippocampal slice culture of 2 WIV and that some of their descendents differentiate into GCL neurons.

Four weeks after retrovirus vector inoculation, about one-quarter of EGFP-expressing cells were immunoreactive with anti-NeuN and about one-quarter with anti-Tuj1, a marker of immature neurons. These numbers compare with those in *in vivo* experiments: 2–25% for anti-NeuN and 15–30% for anti-Tuj1, although these values do depend on the

behavioural conditions of the mice (van Praag *et al.*, 2002). The EGFP-expressing NeuN-positive cells were found primarily in the GCL of the slice culture (Fig. 6A and B). Similarly, most of the BrdU-labelled NeuN-positive cells were found in the GCL, being consistent with the previous study (Raineteau *et al.*, 2004). Therefore, the newly generated neurons are distributed similarly to that reported in postnatal mammals *in vivo* (Kuhn *et al.*, 1996; Eriksson *et al.*, 1998; Kornack & Rakic, 1999). We also found that some EGFP-expressing cells were immunoreactive to calbindin D28K, a marker of GCL neurons (Fig. 6E), being consistent with the *in vivo* studies (Kuhn *et al.*, 1996).

In the adult rodent brain, neurogenic stem cells are present in the subgranular zone of the hippocampus and the newly generated neurons preferentially distribute close to the subgranular zone in the GCL *in vivo* (Cameron *et al.*, 1993; Alvarez-Buylla & Lim, 2004) and in the thin slice culture using the roller-tube methods (Raineteau *et al.*, 2004). However, in our rather thick slice culture system using the interface methods (Stoppini *et al.*, 1991) we found no particular patterns in the appearance of BrdU-labelled/EGFP-expressing NeuN-positive cells in the GCL. Therefore, the three-dimensional structure of the neurogenic niche appears to be somewhat reorganized in our slice culture system.

Undifferentiated cells

One week after mitosis the large number of BrdU-labelled cells appeared to be undifferentiated because they were coexpressing with neither neuronal markers such as NeuN and MAP2 nor astrocyte markers such as GFAP (Fig. 3). Four weeks after retrovirus vector inoculation the EGFP-expressing cells consisted of various phenotypes: NeuN-positive (Fig. 6C); Tuj1-positive (Fig. 6D); GFAP-positive; and nestin-positive (see Supplementary material). Immediately after mitosis the descendants express nestin, an intermediate filament protein found in neuroepithelial stem cells, but usually lose it within a week during maturation (Palmer *et al.*, 2000). Therefore, those nestin-postive EGFP-expressing cells may have a history of recent mitosis. Although we did not investigate phenotypes of nestin-negative EGFP-expressing cells, neuronal and glial progenitors, microglia, endothelial cells and fibroblasts would be included (Raineteau *et al.*, 2004).

Neurons have been shown to express Tuj1 early in differentiation (Lee *et al.*, 1990; Menezes & Luskin, 1994) whereas they express NeuN after maturation (Mullen *et al.*, 1992). Some of our EGFP-expressing neurons showed phenotypes of either early or late stages of differentiation. It is, therefore, possible that there are lineages of self-renewing neural precursor cells that are neurogenic (Palmer *et al.*, 1997) as a consequence of asymmetric cell division (Alvarez-Buylla *et al.*, 2001; Fishell & Kriegstein, 2003). Alternatively, neurons might remain undifferentiated for weeks, and become mature by triggering signals, e.g. synaptic contacts. It is also possible that some of newly generated cells undergo apotosis before maturation (Gould & Gross, 2002) although the EGFP-expressing cells have a tendency to increase in number as a whole as late as 4 weeks after transduction (Fig. 5). Careful follow up of a single pair of EGFP-expressing cells in the slice culture system would shed light on this problem.

Gliogenesis in the slice culture system

Some BrdU-labelled cells expressed GFAP, a molecular marker of astrocytes (Fig. 4C) and about one-third of the EGFP-expressing cells were also positive for GFAP 4 weeks after retrovirus vector inoculation (see Supplementary material). These observations are consistent with previous *in vivo* experiments that cells positive for both BrdU and GFAP are present in the dentate hilus–subgranular zone in the hippocampus (Kempermann *et al.*, 1997). However, the GFAP-positive cells encompass a diverse group of cells (Seri *et al.*, 2001) including terminally differentiated astrocytes (Goldman, 2003) and radial glial cells, which have neurogenic potential (Seri *et al.*, 2001). It has been also suggested that neural precursor cells generally have a history of expressing GFAP at least once (Seri *et al.*, 2001; Kronenberg *et al.*, 2003). Experiments using other molecular markers are necessary to further classify these GFAP-positive cells.

There remains another issue as to whether the GFAP-positive cells and the NeuN-positive cells derived from the same progenitor. This could be tested in our slice culture system by following up a single pair of EGFP-expressing cells using retrovirus vector transduction.

Concluding remarks

Two independent studies, ours and that of Raineteau *et al.* (2004) would make it unequivocal that endogenous neural progenitor cells are indeed present in the slice culture system and spontaneously generating new neurons postnatally. Using the retrovirus vector transduction method in combination, the slice culture system would enable follow up of the newly divided cells for a long period.

Supplementary material

The following supplementary material may be found on: http://www.blackwellpublishing.com/products/journals/suppmat/EJN/EJN3721/EJN3721sm.htm

Fig. S1. Emergence of non-neuronal phenotypes in EGFP-expressing cells in the dentate gyrus around the suprapyramidal region of the GCL after retrovirus vector inoculation.

Acknowledgements

We are grateful to H. Minami for technical assistance R. Araki and K. Miyazaki for helpful comments and to M. Ohara (Fukuoka) for language assistance.

Abbreviations

BrdU, 5-bromodeoxyuridine; DIV, days *in vitro*; EGFP, enhanced green fluorescent protein; GFAP, glial fibrillary acidic protein; GCL, granule cell layer; MAP2, microtubule-associated protein 2; MF, mossy fibre; NeuN, neuronal nuclei antigen; PCL, pyramidal cell layer; TSQ, *N*-(6-methoxy-8-quinolyl)-*p*-toluenesulphonamide; Tuj1, neuron-specific β-III tubulin; WIV, weeks *in vitro*.

References

Altman, J. & Das, G.D. (1965) Autoradiographic and histological evidence of postnatal hippocampal neurogenesis in rats. *J. Comp. Neurol.*, **124**, 319–336.

Alvarez-Buylla, A., Garcia-Verdugo, J.M. & Tramontin, A.D. (2001) A unified hypothesis on the lineage of neural stem cells. *Nat. Rev. Neurosci.*, **2**, 287–293.

Alvarez-Buylla, A. & Lim, D.A. (2004) For the long run: maintaining germinal niches in the adult brain. *Neuron*, **41**, 683–686.

An, D.S., Koyanagi, Y., Zhao, J.-Q., Akkina, R., Bristol, G., Yamamoto, N., Zack, J.A. & Chen, I.S.Y. (1997) High-efficiency transduction of human lymphoid progenitor cells and expression in differentiated T cells. *J. Virol.*, **71**, 1397–1404.

An, D.S., Morizono, K., Li, Q.X., Mao, S.H., Lu, S. & Chen, I.S. (1999) An inducible human immunodeficiency virus type 1 (HIV-1) vector which effectively suppresses HIV-1 replication. *J. Virol.*, **73**, 7671–7677.

Baimbridge, K.G. & Miller, J.J. (1982) Immunohistochemical localization of calcium-binding protein in the cerebellum, hippocampal formation and olfactory bulb of the rat. *Brain Res.*, **245**, 223–229.

Benninger, F., Beck, H., Wernig, M., Tucker, K.L., Brustle, O. & Scheffler, B. (2003) Functional integration of embryonic stem cell-derived neurons in hippocampal slice cultures. *J. Neurosci.*, **23**, 7075–7083.

Bernhardt, R. & Matus, A. (1984) Light and electron microscopic studies of the distribution of microtubule-associated protein 2 in rat brain: a difference between dendritic and axonal cytoskeletons. *J. Comp. Neurol.*, **226**, 203–221.

Bousez-Dumesnil, N., Thomasset, M. & Ben-Ari, Y. (1989) Calbindin-D28K in hippocampal organotypic cultures. *Brain Res.*, **486**, 165–169.

Buchs, P.-A., Stoppini, L. & Muller, D. (1993) Structural modification associated with synaptic development in area CA1 of rat hippocampal organotypic cultures. *Dev. Brain Res.*, **71**, 81–91.

Cameron, H.A., Woolley, C.S., McEwen, B.S. & Gould, E. (1993) Differentiation of newly born neurons and glia in the dentate gyrus of the adult rat. *Neuroscience*, **56**, 337–344.

Dailey, M.E., Buchanan, J., Bergles, D.E. & Smith, S.J. (1994) Mossy fiber growth and synaptogenesis in rat hippocampal slices in vitro. *J. Neurosci.*, **14**, 1060–1078.

Dayer, A.G., Ford, A.A., Cleaver, K.M., Yassaee, M. & Cameron, H.A. (2003) Short-term and long-term survival of new neurons in the rat dentate gyrus. *J. Comp. Neurol.*, **460**, 563–572.

Eriksson, P.S., Perfilieva, E., Bjork-Eriksson, T., Alborn, A.-M., Nordborg, C., Peterson, D.A. & Gage, F.H. (1998) Neurogenesis in the adult human hippocampus. *Nat. Med.*, **4**, 1313–1317.

Fishell, G. & Kriegstein, A.R. (2003) Neurons from radial glia: the consequences of asymmetric inheritance. *Curr. Opin. Neurobiol.*, **13**, 34–41.

Frederickson, C.J., Kasarskis, E.J., Ringo, D. & Frederickson, R.E. (1987) A quinoline fluorescence method for visualizing and assaying the histochemically reactive zinc (bouton zinc) in the brain. *J. Neurosci. Meth.*, **20**, 91–103.

Frederickson, C.J., Suh, S.W., Silva, D., Frederickson, C.J. & Thompson, R.B. (2000) Importance of zinc in the central nervous system: the zinc-containing neuron. *J. Nutr.*, **130** (suppl.), 1471S–1483S.

Gähwiler, B.H. (1984) Development of the hippocampus in vitro: cell types, synapses and receptors. *Neuroscience*, **11**, 751–760.

Gähwiler, B.H., Capogna, M., Debanne, D., McKinney, R.A. & Thompson, S.M. (1997) Organotypic slice cultures: a technique has come of age. *Trends Neurosci.*, **20**, 471–477.

Goldman, S. (2003) Glia as neural progenitor cells. *Trends Neurosci.*, **26**, 590–596.

Gould, E., Beylin, A., Tanapat, P., Reeves, A. & Shors, T.J. (1999a) Learning enhances adult neurogenesis in the hippocampal formation. *Nat. Neurosci.*, **2**, 260–265.

Gould, E. & Gross, D.G. (2002) Neurogenesis in adult mammals: some progress and problems. *J. Neurosci.*, **22**, 619–623.

Gould, E., Reeves, A.J., Fallah, M., Tanapat, P. & Gross, C.G. (1999b) Hippocampal neurogenesis in adult Old World primates. *Proc. Natl. Acad. Sci. USA*, **96**, 5263–5267.

Gould, E. & Tanapat, P. (1997) Lesion-induced proliferation of neuronal progenitors in the dentate gyrus of the adult rat. *Neuroscience*, **80**, 427–436.

Gutierrez, R. & Heinemann, U. (1999) Synaptic reorganization in explanted cultures of rat hippocampus. *Brain Res.*, **815**, 304–316.

Hastings, N.B. & Gould, E. (1999) Rapid extension of axons into the CA3 region by adult-generated granule cells. *J. Comp. Neurol.*, **413**, 146–154.

Hayes, N.L. & Nowakowski, R.S. (2002) Dynamics of cell proliferation in the adult dentate gyrus of two inbred strains of mice. *Dev. Brain Res.*, **134**, 77–85.

Henze, D.A., Urban, N.N. & Barrionuevo, G. (2000) The multifarious hippocampal mossy fiber pathway: a review. *Neuroscience*, **98**, 407–427.

Kempermann, G. (2002) Why new neurons? Possible functions for adult hippocampal neurogenesis. *J. Neurosci.*, **22**, 635–638.

Kempermann, G., Kuhn, H.G. & Gage, F.H. (1997) More hippocampal neurons in adult mice living in an enriched environment. *Nature*, **386**, 493–495.

Kornack, D.R. & Rakic, P. (1999) Continuation of neurogenesis in the hippocampus of the adult macaque monkey. *Proc. Natl. Acad. Sci. USA*, **96**, 5768–5773.

Kronenberg, G., Reuter, K., Steiner, B., Brandt, M.D., Jessberger, S., Yamaguchi, M. & Kempermann, G. (2003) Subpopulations of proliferating cells of the adult hippocampus respond differently to physiologic neurogenic stimuli. *J. Comp. Neurol.*, **467**, 455–463.

Kuhn, H.G., Dickinson-Anson, H. & Gage, F.H. (1996) Neurogenesis in the dentate gyrus of the adult rat: age-related decrease of neuronal progenitor proliferation. *J. Neurosci.*, **16**, 2027–2033.

Kuhn, H.G., Palmer, T.D. & Fuchs, E. (2001) Adult neurogenesis: a compensatory mechanism for neuronal damage. *Eur. Arch. Psychiatry Clin. Neurosci.*, **251**, 152–158.

Landau, N.R. & Littman, D.R. (1992) Packaging system for rapid production of murine leukemia virus vectors with variable tropism. *J. Virol.*, **66**, 5110–5113.

Lee, M.K., Rebhun, L.I. & Frankfurter, A. (1990) Posttranslational modification of class III beta-tubulin. *Proc. Natl. Acad. Sci. USA*, **87**, 7195–7199.

Lendahl, U., Zimmerman, L.B. & McKay, R.D. (1990) CNS stem cells express a new class of intermediate filament protein. *Cell*, **60**, 585–595.

Liu, J., Solway, K., Messing, R.O. & Sharp, F.R. (1998) Increased neurogenesis in the dentate gyrus after transient global ischemia in gerbils. *J. Neurosci.*, **18**, 7768–7778.

Ludwin, S.K., Kosek, J.C. & Eng, L.F. (1976) The topographical distribution of S-100 and GFA proteins in the adult rat brain: an immunohistochemical study using horseradish peroxidase-labelled antibodies. *J. Comp. Neurol.*, **165**, 197–207.

Markakis, E.A. & Gage, F.H. (1999) Adult-generated neurons in the dentate gyrus send axonal projections to field CA3 and are surrounded by synaptic vesicles. *J. Comp. Neurol.*, **406**, 449–460.

Menezes, J.R. & Luskin, M.B. (1994) Expression of neuron-specific tubulin defines a novel population in the proliferative layers of the developing telencephalon. *J. Neurosci.*, **14**, 5399–5416.

Miyaguchi, K. (1997) Ultrastructure of intermediate filaments of nestin- and vimentin-immunoreactive astrocytes in organotypic slice cultures of hippocampus. *J. Struct. Biol.*, **120**, 61–68.

Mullen, R.J., Buck, C.R. & Smith, A.M. (1992) NeuN, a neuronal specific nuclear protein in vertebrates. *Development*, **116**, 201–211.

Okada, M., Sakaguchi, T. & Kawasaki, K. (1995) Correlation between anti-ubiquitin immunoreactivity and region-specific neuronal death in *N*-methyl-D-aspartate-treated rat hippocampal organotypic cultures. *Neurosci. Res.*, **22**, 359–366.

Palmer, T.D., Takahashi, J. & Gage, F.H. (1997) The adult rat hippocampus contains primordial neural stem cells. *Mol. Cell. Neurosci.*, **8**, 389–404.

Palmer, T.D., Willhoite, A.R. & Gage, F.H. (2000) Vascular niche for adult hippocampal neurogenesis. *J. Comp. Neurol.*, **425**, 479–494.

van Praag, H., Schinder, A.F., Christie, B.R., Toni, N., Palmer, T.D. & Gage, F.H. (2002) Functional neurogenesis in the adult hippocampus. *Nature*, **415**, 1030–1034.

Raineteau, O., Rietschin, L., Gradwohl, G., Guillemot, F. & Gähwiler, B.H. (2004) Neurogenesisi in hippocampal slice cultures. *Mol. Cell. Neurosci.*, **26**, 241–250.

Rakic, P. (2002) Adult neurogenesis in mammals: An identity crisis. *J. Neurosci.*, **22**, 614–618.

Robain, O., Barbin, G., Billette de Villemeur, T., Jardin, L., Jahchan, T. & Ben-Ari, Y. (1994) Development of mossy fiber synapses in hippocampal slice culture. *Dev. Brain Res.*, **80**, 244–250.

Sakaguchi, T., Okada, M. & Kawasaki, K. (1994) Sprouting of CA3 pyramidal neurons to the dentate gyrus in rat hippocampal organotypic cultures. *Neurosci. Res.*, **20**, 157–164.

Seri, B., Garcia-Verdugo, J.M., McEwen, B.S. & Alvarez-Buylla, A. (2001) Astrocytes give rise to new neurons in the adult mammalian hippocampus. *J. Neurosci.*, **21**, 7153–7160.

Shors, T.J., Miesegaes, G., Beylin, A., Zhao, M., Rydel, T. & Gould, E. (2001) Neurogenesis in the adult is involved in the formation of trace memories. *Nature*, **410**, 372–376.

Song, H.-J., Stevens, C.F. & Gage, F.H. (2002) Neural stem cells from adult hippocampus develop essential properties of functional CNS neurons. *Nat. Neurosci.*, **5**, 438–445.

Stoppini, L., Buchs, P.A. & Muller, D. (1991) A simple method for organotypic cultures of nervous tissue. *J. Neurosci. Meth.*, **37**, 173–182.

Tamamaki, N., Nakamura, K., Furuta, T., Asamoto, K. & Kaneko, T. (2000) Neurons in Golgi-stain-like images revealed by GFP-adenovirus infection in vivo. *Neurosci. Res.*, **38**, 231–236.

Varea, E., Ponsoda, X., Molowny, A., Danscher, G. & Lopez-Garcia, C. (2001) Imaging synaptic zinc release in living nervous tissue. *J. Neurosci. Meth.*, **110**, 57–63.

Vogt, K., Mellor, J., Tong, G. & Nicoll, R. (2000) The actions of synaptically released zinc at hippocampal mossy fiber synapses. *Neuron*, **26**, 187–196.

Zimmer, J. & Gähwiler, B.H. (1984) Cellular and connective organization of slice cultures of the rat hippocampus and fascia dentata. *J. Comp. Neurol.*, **228**, 432–446.

Zufferey, R., Nagy, D., Mandel, R.J., Naldini, L. & Trono, D. (1997) Multiply attenuated lentiviral vector achieves efficient gene delivery in vivo. *Nat. Biotechnol.*, **15**, 871–875.

AIDS RESEARCH AND HUMAN RETROVIRUSES
Volume 20, Number 3, 2004, pp. 337–340

Sequence Note

Determination of HIV Type 1 CRF01_AE gag p17 and env-V3 Consensus Sequences for HIV/AIDS Vaccine Design

TAKAICHI HAMANO,[1] PATHOM SAWANPANYALERT,[2] HIDEKI YANAI,[1,3] SURACHAI PIYAWORAWONG,[4] TAKASHI HARA,[5] SOMPONG SAPSUTTHIPAS,[1] JURAIRAT PHROMJAI,[2] SHUDO YAMAZAKI,[1,5] NAOKI YAMAMOTO,[5] PAIJIT WARACHIT,[6] MITSUO HONDA,[1,5] and KAZUHIRO MATSUO[1,5]

ABSTRACT

A molecular epidemiological study of the gag p17 and env-V3 regions on HIV-infected drug users and blood donors was carried out in northern Thailand from 1998 through 2002 to determine the predominant subtype and consensus sequence (CS) for circulating HIV-1 strains. CRF01_AE was concluded to be a predominant strain and the nucleotide CSs in gag p17 and env-V3 showed only 1.26% and no difference from CS in the Los Alamos database, respectively. Our env-V3 CS was identical to the previously published CSs, suggesting that the CS was very conserved from 1990 through 2002 in Thailand. Gag p17 and env-V3 nucleotide sequences of seroconvertors in our subjects were quite similar to the CS and conserved for at least 9 and 6 years postinfection, respectively. These results suggest that the CS approach to the HIV-1 antigen design could overcome HIV diversity and help us develop an effective HIV/AIDS vaccine.

THE ANTIGEN GENES IN THE FIRST-GENERATION HIV/AIDS CANDIDATE VACCINES were obtained from isolated viruses. However, the range of amino acid (AA) changes of each isolate demonstrated more than 30% difference from the CRF01_AE consensus envelope sequence.[1] Considering the diversity of each circulating virus, investigators find it very difficult to select an optimal antigen from numerous isolates to develop an efficacious preventive HIV/AIDS vaccine. Currently, three computational methods (consensus, ancestral, and center of the tree) are being considered as a strategy for a novel antigen design of an HIV/AIDS vaccine to overcome HIV diversity.[1,2] However, these novel types of antigen have never been used for vaccine construction to control the HIV-1 CRF01_AE epidemic in Thailand. From 1998 to 2002, to characterize currently circulating viruses in northern Thailand, we determined HIV-1 subtypes among HIV-1-seropositive drug users (DUs) and blood donors (BDs) in Chiang Rai in northern Thailand using provirus sequences of gag p17 and env-V3 regions. Furthermore, CSs of both regions were classified and compared with those in the database,[3] in 1990s isolated samples[4] and in seroconvertors,[5] respectively.

One hundred and nineteen HIV-1-infected DUs and 96 BDs were investigated. Their $CD4^+$ and $CD8^+$ T lymphocyte absolute count indicated a mean value of 308/μl (range: 8–1449/μl) and 747/μl (range: 98–3079μl) in DU, respectively. Phylogenetic tree analysis of the gag p17 and env-V3 regions revealed that the predominant HIV-1 subtype was CRF01_AE with 88% and 97% in the DU and BD groups, respectively (data not shown). Other minor subtypes were classified as B′ (Thailand variant of subtype B) and B in the both groups.

CSs of the CRF01_AE gag p17 (CSg) and env-V3 (CSe) regions were determined using proviral sequences derived from

[1]JST AIDS Vaccine Project, c/o National Institute of Health, Ministry of Public Health, Nonthaburi 11000, Thailand.
[2] National Institute of Health, Ministry of Public Health, Nonthaburi 11000, Thailand.
[3]TB/HIV Research Project, RIT-JATA, Muang District, Chiang Rai 57000, Thailand.
[4]Mae Chan Hospital, Mae Chan district, Chiang Rai 57110, Thailand.
[5]National Institute of Infectious Diseases, Japan, Tokyo 162-8640, Japan.
[6]Ministry of Public Health, Thailand, Nonthaburi 11000, Thailand.

35 and 126 individuals, respectively. These CSs were compared to the available CRF01_AE CS (CSD) in the database (Table 1).[3] In the gag p17 region, nucleotide sequence and AA alignment difference showed means of 2.66 and 5.11% from our CSg, respectively. CSg showed a difference of 1.26% in nucleotides and 3.79% in AA, as compared with CSD.[3] The average magnitude (n = 16) of the gag p17 nucleotide and AA difference between CSg and each isolate in Table 1 showed no significant difference from circulating viruses in our specimens (Student's t test). Furthermore, CSg and CSD of gag p17 were close to the isolates prior to 1993 than to those after 1994.

In the case of the env-V3 region, the mean differences of our nucleotide and AA sequences from CSe were 5.55 and 11.59%, respectively. The CSe of nucleotide and AA sequences were

TABLE 1. COMPARISON OF OUR CONSENSUS SEQUENCES WITH DATABASE OF HIV-1 CRF01_AE gag P17 AND env-V3[a]

	Compared to our CS of gag p17		*Compared to our CS of env-V3*	
Sample name	*Different nuc (%)*	*Different AA (%)*	*Different nuc (%)*	*Different AA(%)*
93TH057	4.55	9.85	7.62	14.29
93TH065	2.27	5.30	0.95	2.86
95TH253	3.03	6.06	12.38	37.14
93TH902	4.29	8.33	7.62	8.57
94TH702	3.03	6.06	No data	No data
94TH7091	3.03	6.06	No data	No data
95TNIH022	3.79	6.82	20.95	42.86
95TNIH047	3.79	7.58	16.19	31.43
97TH6-107	3.54	6.06	0.95	0.00
CM235	1.26	2.27	2.86	5.71
CM238	1.77	4.55	0.95	2.86
CM239	No data	No data	0.95	2.86
CM240	2.27	5.30	2.86	5.71
CM241	No data	No data	0.00	0.00
CM242	No data	No data	0.95	2.86
CM243	1.01	1.52	5.71	14.29
CM244	No data	No data	0.00	0.00
TN240	1.52	3.79	No data	No data
TN245	2.02	3.03	No data	No data
92TH022	1.01	2.27	0.95	2.86
CS from database[3]	1.26	3.79	0.00	0.00
CS from McCutchan *et al.*[4]	No data	No data	0.00	0.00
CS from Subbarao *et al.*[5]	No data	No data	0.00	0.00
Calculated by above samples				
Mean (n = 16)	2.64	5.30	5.12	10.89
Range	1.01–4.55	1.52–9.85	0–20.95	0–42.86
Calculated by our samples				
Mean (n = gag p17, env-V3 = 35,126)	2.66	5.11	5.55	11.59
Range	0.76–4.80	2.27–9.73	0–15.24	0–40.00
Calculated by seroconvertors' samples[5]				
Mean (n = 102)	No data	No data	3.14[b]	6.49[b]
Range	No data	No data	0–11.43	0–22.86
Years after seroconversion in our samples				
<1: Mean (n = gag p17, env-V3 = 9, 13)	3.17	4.80	4.91	9.67
Range	1.52–5.05	1.52–6.82	0.95–7.62	2.83—17.14
1–3: Mean (n = gag p17, env-V3 = 0, 12)	No sample	No sample	5.16	9.29
Range			1.90–0.48	2.86–17.14
3–6: Mean (n = gag p17, env-V3 = 9, 21)	2.40	4.58	5.62	12.24
Range	0.76–4.13	2.27–7.03	0.95–15.24	2.86–31.43
>6–9: Mean (n = gag p17, env-V3 = 9, 12)	2.81	6.05	7.70[c]	17.38[d]
Range	1.52–4.29	3.03–9.73	1.90–14.29	2.86–31.43

[a]CS, consensus sequence; nuc, nucleotide; AA, amino acid.
[b]Significantly different from our samples ($p < 0.0001$).
[c,d]Significantly different from <1 sample (p = 0.038 and 0.010).

identical to those of CSD. The average distance (n = 16) of the env-V3 nucleotide and AA sequence of each isolate in the database[3] from CSe was 5.12 and 10.89%, respectively, and they showed no significant differences from circulating viruses in our specimens. CSs of nucleotide and AA of env-V3 in seroconvertors[5] who were infected during 1995–1998 were also identical to CSe. However, there was an average of 3.14% in nucleotide and 6.49% in AA differences that were significantly closer to CSe than to other available sequences. Furthermore, the CS of env-V3 that was determined by six specimens (CM235–CM244) isolated in 1990 in northern Thailand[4] was identical to CSe. 93TH065[6] and 92TH022[7] isolated from early seroconvertors indicated high similarity to CSs in both regions.

From our investigation, it was revealed that the consensus nucleotide and AA sequences of env-V3 in circulating CRF01_AE were very conserved from 1990 through 2002 in Thailand[4,5,7–9] and that the nucleotide sequence distance in the C2–V3 region from seroconvertors in DU was low[5] and each isolate was more similar to the env-V3 CS than our isolates. In addition, seven of 102 samples in DU seroconvertors in Bangkok[5] and two of six CM series samples[4] showed quite high homogeneity to CSe. In our subjects, 27 of 35 in gag p17 and 58 of 126 in env-V3 had definitive risk for HIV-1 infection from the data of Sawanpanyalert *et al.*[10–12] and were divided into four groups by year after seroconversion (less than 1 year, 1–3 years, 3–6 years, and >6–9 years). Using nucleotide and AA sequences in both regions, we compared seroconvertors (less than 1 year) with other year groups and with seroconvertors in a Bangkok DU cohort[5] as an env-V3 control. The sequence differences in gag p17 and env-V3 were not statistically significant among all year groups or the Bangkok DU group except for the >6–9 years group, which showed significant difference (p = 0.038 in nucleotide and 0.010 in AA levels), suggesting that seroconvertors possessed a quite similar sequence and maintained the similarity for at least 6 years. These results suggest that the CRF01_AE sequence was conserved for quite a long time and a certain specific type of virus whose sequence is close to the CS might be the one that is mainly transmitted. Furthermore, taking account of the high homogeneity of our CSs to the early isolates during the pandemic in Thailand (93TH065, 92TH022, and CM series), CRF01_AE has not been evolving in a unique direction but at random and then consequently conserves its CSs, as compared to the sequence of isolates in the pandemic stage.

As for another subtype, the env and gag AA sequences in HIV-1 subtype C isolates shared identity 92–95% and 90.5–98.7% with the South African CS, respectively.[13] Subtype C gag p17 and p24 AAs were relatively conserved and showed less than 10% diversity to CS in Botzwana.[14] Abidjan AA CS of gag p24 was 99.32% identical to reference CRF02_AG.[15] The 4 incidence and 19 prevalence cases were 97.1 and 96.6% homologous to Abidjan CS, respectively, and the range in incidence cases was narrower than that in prevalence cases.[15] These results suggest that the CS could provide a less distant virus sequence in the population than each circulating isolate even in the different subtypes.

In summary, a consensus approach for antigen genes could minimize the sequence distance from each circulating isolate and may provide an effective strategy to construct an HIV/AIDS vaccine candidate that could induce broad protective efficacy against diverse HIV-1 isolates.

ACCESSION NUMBERS

gag p17: AB115505–AB115540; env-V3: AB115782–AB115907.

ACKNOWLEDGMENTS

We gratefully acknowledge the dedicated field work of Ms. Saiyud Moolphate, Ms. Pornpimon Saksoong, and other members of the TB/HIV Research Project, the RIT-JATA, the Regional Medical Sciences Centre in Chiang Rai, and the Mae Chan Hospital. We also thank Dr. Kruavon Balachandra for her kind technical support and advice. This investigation was cosponsored by grants from the Sasakawa Memorial Health Foundation, the Japanese Foundation for AIDS Prevention, and the Japan Health Sciences Foundation.

REFERENCES

1. Gaschen B, Taylor J, Yusim K, *et al.*: Diversity considerations in HIV-1 vaccine selection. Science 2002;296:2354–2360.
2. Nickle DC, Jensen MA, Gottlieb GS, *et al.*: Consensus and ancestral state HIV vaccines. Science 2003;299:1515–1518.
3. Korber B, Brander C, Haynes BF, et al. (eds.): *HIV Immunology and Sequence Databases.* Los Alamos National Laboratory, Los Alamos, NM, 2003.
4. McCutchan FE, Hegerich PA, Brennan TP, *et al.*: Genetic variants of HIV-1 in Thailand. AIDS Res Hum Retroviruses 1992;8: 1887–1895.
5. Subbarao S, Vanichseni S, Hu DJ, *et al.*: Genetic characterization of incident HIV type 1 subtype E and B strains from a prospective cohort of injecting drug users in Bangkok, Thailand. AIDS Res Hum Retroviruses 2000;16:699–707.
6. Anderson JP, Rodrigo AG, Learn GH, *et al.*: Testing the hypothesis of a recombinant origin of human immunodeficiency virus type 1 subtype E. J Virol 2000;74:10752–10765.
7. WHO Network for HIV Isolation and Characterization: HIV type 1 variation in World Health Organization-sponsored vaccine evaluation sites: Genetic screening, sequence analysis, and preliminary biological characterization of selected viral strains. AIDS Res Hum Retroviruses 1994;10:1327–1343.
8. Kalish ML, Baldwin A, Raktham S, *et al.*: The evolving molecular epidemiology of HIV-1 envelope subtypes in injecting drug users in Bangkok, Thailand: Implications for HIV vaccine trials. AIDS 1995;9:851–857.
9. Tian H, Lan C, and Chen YH: Sequence variation and consensus sequence of V3 loop on HIV-1 gp120. Immunol Lett 2002;83: 231–233.
10. Sawanpanyalert P, Supawitkul S, Yanai H, Saksoong P, and Piyaworawong S: Trend of HIV infection rates among drug users in an HIV epicenter in northern Thailand (1989–1997). J Epidemiol 1999;9:114–120.
11. Jittiwutikarn J, Sawanpanyalert P, Rangsiveroj N, and Satitvipawee P: HIV incidence rates among drug users in northern Thailand, 1993–7. Epidemiol Infect 2000;125:153–158.

12. Sawanpanyalert P, Yanai H, Kitsuwannakul S, and Nelson KE: An estimate of the number of human immunodeficiency virus (HIV)-positive blood donations by HIV-seronegative donors in a northern Thailand HIV epicenter. J Infect Dis 1996;174:870–873.
13. Williamson C, Morris L, Maughan MF, *et al.*: Characterization and selection of HIV-1 subtype C isolates for use in vaccine development. AIDS Res Hum Retroviruses 2003;19:133–144.
14. Novitsky V, Smith UR, Gilbert P, *et al.*: Human immunodeficiency virus type 1 subtype C molecular phylogeny: Consensus sequence for an AIDS vaccine design? J Virol 2002;76:5435–5451.
15. Ellenberger DL, Li B, Lupo LD, *et al.*: Generation of a consensus sequence from prevalent and incident HIV-1 infections in West Africa to guide AIDS vaccine development. Virology 2002;302:155–163.

Address reprint requests to:
Takaichi Hamano
JST AIDS Vaccine Project
c/o National Institute of Health
Ministry of Public Health
88/7 Soi Bamrasnaradura
Tivanond Road
Nonthaburi 11000, Thailand

E-mail: taka0627@yahoo.co.jp
or hamano@dmsc.moph.go.th

Exp. Anim. 53(4), 321–329, 2004

The Normalization of Guinea Pig Leukocyte Fractions and Lymphocyte Subsets in Blood and Lymphoid Tissues using a Flow Cytometric Procedure

Mari TAKIZAWA[1,4], Jo CHIBA[5], Shinji HAGA[2], Toshihiko ASANO[3], Naoki YAMAMOTO[1], and Mitsuo HONDA[1]

[1]AIDS Research Center, [2]Department of Bacteriology, [3]Division of Experimental Animal Research, National Institute of Infectious Diseases, 1–23–1 Toyama, Shinjuku-ku, Tokyo, 162-8640, [4]Japan Health Science Foundation, 13–4 Nihonbashi Kodenma-cho, Chuo-ku, Tokyo, 103-0001, and [5]Faculty of Industrial Science and Technology, Tokyo University of Science, 2669 Yamazaki, Noda-shi, Chiba, 278-0022 Japan

Abstract: *Many hematological and immunological parameters remain unclear in the study of the guinea pig. In this study, we established the mean values of blood counts, the percentage of leukocyte fractions and lymphocyte subsets in blood and various lymphoid tissues of the guinea pig with a flow cytometric procedure using MIL4/SSC. The mean counts of WBC and RBC in the blood were lower, and MCV and MCH were higher than those of other rodents, resembling those of humans. Furthermore, the mean percentages of blood lymphocytes were smaller and that of granulocyte was larger than those of other rodents, resembling those of humans. We further established a flow cytometric procedure for lymphocyte subsets and clarified the mean percentages of T- and B-cells, CD4+-, CD8+- and MHC Class II+- T-cells, and CD4-CD8- T-cells. The latter were morphologically larger in cell size and cytoplasm than CD4+- plus CD8+ T-cells, and this subset had a significantly higher percentage in newborn animals. Furthermore, the appearance of the MHC Class II+ T-cell subset was suggested to be a marker of hyper-activation of T-cells in BCG-immunized animals. Thus, both the novel flow cytometric procedure for leukocyte fractions and lymphocyte subsets, and the established normal values will be useful tools in studying guinea pigs as models of various diseases and biological phenomena.*

Key words: *flow cytometry, guinea pig, immunological values, leukocyte fraction, T-cell subpopulation*

Introduction

The guinea pig has been a widely used experimental animal for studies on human tuberculosis and other mycobacterial infections because of the particular susceptibility of this species to *Mycobacterium tuberculosis* [15]. Furthermore, vaccinating guinea pigs with *Mycobacterium bovis* Bacillus Calmette-Guérin (BCG) has

(Received 19 November 2003 / Accepted 2 March 2004)

Address corresponding: M. Honda, AIDS Research Center, National Institute of Infectious Diseases, 1–23–1 Toyama, Shinjuku-ku, Tokyo, 162-8640, Japan

several important advantages over vaccinating mice such as delayed-type hypersensitivity skin reactions (DTH) to PPD and development of lesions that are similar to those induced in humans [1]. Moreover, the animal has been also used as an animal model for syphilis [30, 31], other genital diseases [6], tinnitus [7, 8, 17], shock [19], allergic diseases [10, 29] and various tumors [5, 22].

Monoclonal antibody and flow cytometric analysis have been widely used to study immunology, pathology and physiology including experimental disease in humans and mice [2, 4]. The number and composition of the blood counts and lymphocyte subsets in the blood and tissue are assumed to be influenced by many factors. However, the precise phenotype of cells and immune responses in the guinea pig have been difficult to analyze because of the limited availability of anti-guinea pig antibodies and animal strains, which remain to be established.

In this study, we devised a flow cytometric method using commercially and personally available antibodies to fractionate guinea pig leukocytes, i.e., lymphocytes, monocytes, granulocytes and Kurloff cell included fractions in the blood and various lymphoid tissues of guinea pigs. Furthermore, we clearly identified T-cells and B-cells, $CD8^+$ T-cells, $CD4^+$ T-cells and MHC Class II^+-activated T-cells, and $CD4^-CD8^-$ T-cell subsets, most of which were compared between adult and newborn guinea pigs. Further, we suggest that the appearance of MHC Class II^+ T-cell subpopulation in BCG-hyperinoculated animals may be a marker of lymphocyte hyperactivation.

Materials and Methods

Animals: Hartley strain guinea pigs were obtained from Japan SLC, Inc., Japan. We used three groups of female guinea pigs. The first group comprised 3 days old guinea pigs (N=12), the second group, 8 weeks old guinea pigs (N=60), and the third group, 2 years old guinea pigs (N=12). The animals were kept in a specific-pathogen-free area according to the Institutional Animal Care and Use Guidelines of the National Institute of Infectious Diseases (NIID), Japan.

Antibodies: This study used FITC-labeled mouse monoclonal antibodies (mAbs) anti-guinea pig CD4 (T helper/inducer, CT7, Serotec Ltd., Kidlington, Oxford, UK), anti-guinea pig CD8 (CT6, Serotec), anti-guinea pig B-cells (Msgp9, Serotec) and anti-guinea pig T-cells (CT5, Serotec) [24, 28], anti-porcine granulocyte (MIL4, Serotec) [25] and anti-guinea pig MHC Class II antigen (27E7) [24], anti-asialo GM1 (Wako Pure Chem.Ldt., Tokyo, Japan) [14], PE-labeled Goat anti-rabbit IgG-$F(ab')_2$ (Caltag Lab., Burlingam, CA), streptavidin-cychrome (Pharmingen, Sam diego, CA) and PE-labeled rabbit anti-mouse IgG-$F(ab')_2$ (Serotec).

Isolation of blood and various tissue cells: Blood cells were hemolized by adding ACK lysis buffer consisting of 0.15 M NH_4Cl, 0.1 mM EDTA-2Na, and 1.0 mM $KHCO_3$ at ratio of 13:1 and incubated for 5 min at RT. The cells were washed twice and were resuspended in a PBS staining buffer with 0.1% NaN_3 and 3% FCS. Splenocytes, lymph node cells and thymocytes were teased out using a mesh filter Cell Strainer (Becton Dickinson Labware, Franklin, NJ) and hemolized by adding ACK lysis buffer. After washing, the cells were resuspended in a PBS staining buffer.

Flow cytometric assay: Three color staining. The cells (5×10^5 cells/50 μl) were incubated with purified antibody at 4°C for 30 min and washed twice with a cold staining buffer. PE-conjugated rabbit anti-mouse IgG $F(ab')_2$ was then added at 4°C for 30 min, and the cells were washed twice with the staining buffer. Finally, the cells were stained with FITC-conjugated antibodies at 4°C for 30 min followed by 2 more washes with the staining buffer.

Four color staining: The cells (5×10^5 cells/50 μl) were incubated with a purified anti-asialo GM1 rabbit antibody at 4°C for 30 min and washed twice with a cold staining buffer. PE-conjugated goat anti-rabbit IgG $F(ab')_2$ was then added at 4°C for 30 min, and the cells were washed twice with the staining buffer. Then, the cells were stained with biotin-conjugated CT7 (CD4) and CT6 (CD8) at 4°C for 30 min followed by 2 washes with the staining buffer. Streptavidin-cychrome (Pharmingen) was added 4°C for 30 min, and the cells were washed twice with the staining buffer. Finally, the cells were stained with FITC-conjugated CT5 (T cell) at 4°C for 30 min followed by 2 more washes. Target cells were stained with respective Abs according to the manufacturer's instruction. To remove dead cells 200 μl of propidium iodide (Sigma Chem. Co., St Louis, USA) at a concentration of 5 μg/ml was added, and viable cells were analyzed on a FACScalibur

Table 1. Panel of anti-guinea pig mAb used in the flow cytometry[a)]

Clone name	Specificity	Sections[b)]	Dye[c)]	Ig class
Msgp9	Pan B-cell	F, C	FITC	IgG
31D2	IgM	F, I	Purify	IgG
CT5	Pan T-cell	F, C, P	FITC, Purify	IgG
MIL4	Porcine neutrophil and eosinophil	F, C	FITC	IgG
CT7	CD4 (T helper/inducer)	F, C	FITC, biotin	IgG
CT6	CD8 (T suppressor/cytotoxic)	F, C	FITC, biotin	IgG
R27E	MHC Class II	F, I	Purify	IgG
Asialo GM1	Mouse and rat NK cells	F, I	Purify	IgG

[a)] Anti-guinea pig mAb R27E was a kind gift from Dr. R. Burger, Robert Koch Institute, Berlin, Germany, and the others were obtained from Serotec. [b)] Method identifying the specificity of mAb: F, flow cytometry; I, immunohistology; C, immunohistology-cryostat; and P, immunohistology-paraffin. [c)] Labeled dye of mAb; FITC, FITC-labeled mAb; Purify, purified mAb; and biotin, biotinylated mAb.

(Becton-Dickinson, San Joes, CA, USA) equipped with an argon laser set at 488 nm using Cell Quest software (Becton-Dickinson). The emission wavelengths used for FITC, PE, PI and cychrome were 530 nm, 580 nm, 610 nm and 630 nm respectively [32, 33]. The viable cells were sorted with a FACS Vantage SE (Becton-Dickinson) equipped with argon, dye and UV lasers.

Differentiation of leukocyte fractions of guinea pig and further study of its lymphocyte subpopulations: Leukocyte of guinea pig was initially gated into 4 fractions by flow cytometry using MIL4/SSC parameter [26]. Then, the lymphocyte fraction of guinea pig gated with another SSC/FSC parameter was adjusted by the results, which were simultaneously obtained with the lymphocyte fraction gated by the MIL4/SSC parameter as described above. The lymphocytes subpopulations were further studied with the adjusted lymphocyte population by using various guinea pig antibodies as described in Table 1. Data were expressed as the mean percent positive cells ± SD.

Blood count: Blood counts were performed according to the manufacturer's instructions with an automated blood analyzer Celltac (Nihon Koden, Tokyo, Japan). Both white and red blood cells of guinea pigs were also counted with a hemacytometer chamber and the results obtained with the two methods described above were confirmed as identical.

Morphological studies: The sorted cells were cytocentrifuged using Cytospin 3 (Shandon, Life Sciences International, Runcorn, UK) and stained with the May-Giemsa solution (Merck KGaA, Darmstadt, Germany) as previously described [21, 33].

Table 2. Mean value of the hemograms of blood sample from normal guinea pigs[a)]

Item	Unit	Mean	SD
RBC	10^4/μl	499	47
WBC	/μl	5,438	1,689
Hb	g/dl	14.7	1.3
Ht	%	43.0	7.8
MVC	fl	87.7	4.9
MCH	pg	29.7	1.4
MCHC	g/dl	33.8	2.3
PLT	10^4/μl	41.7	10.5

[a)] Data are expressed as the mean ± SD. N=60.

Statistical analysis: Calculations were performed to determine the geometric mean ± SD. Statistical comparisons were performed using Student's *t*-test. Statistical significance was defined as $P<0.05$.

Results

Mean values of the blood counts of the guinea pigs

We initially determined the mean values of the hemograms of heart-punctured blood samples from 60 Hartley guinea pigs with 8 weeks old weighing 400 g by adjusting the automated blood analyzer to study guinea pig blood samples (Table 2). The mean absolute counts of white blood cells (WBC), red blood cells (RBC) and platelets (PLT) were 5438 ± 1689, 499 × 10^4 ± 47 and 41.7 × 10^4 ± 10.5/μl, respectively. The

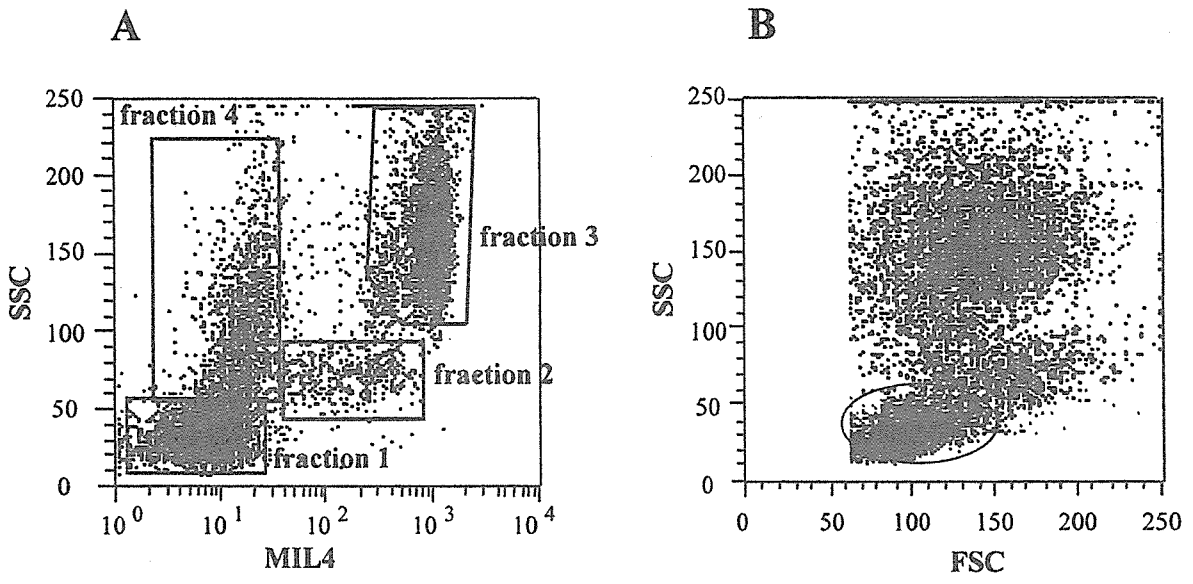

Fig. 1. The leukocyte fractions in various lymphoid tissues of guinea pigs using flow cytometry. (A) Two-color analysis was performed with the leukocytes of lymphoid tissues. Dead cells were removed by propidium iodide and viable cells were differentiated with MIL4/SSC. Fraction 1, lymphocyte population (Green dots); fraction 2, monocyte population; fraction 3, granulocyte population; and fraction 4, Kurloff cell-containing population. (B) Accurate gating of the lymphocyte population reflected by MIL4/SSC flow cytometry for the lymphocyte fraction described above. The green dots show the lymphocyte population by gating with FSC/SSC. Two color flow cytometry was applied to the gated lymphocyte population to study lymphocyte subsets and subpopulations.

mean values of hemoglobin concentration (Hb), hematocrit (Ht), mean corpuscular volume (MCV), mean corpuscular hemoglobin (MCH), and mean corpuscular hemoglobin concentration (MCHC) were 14.7 ± 1.3 g/dl, 43.0 ± 7.8%, 87.7 ± 4.9 fl, 29.7 ± 1.4 pg, and 33.8 ± 2.3 g/dl, respectively.

Gating of WBC fractions by flow cytometric analysis using MIL4/SSC

One problem in studying immunological reactions in guinea pigs is due to difficulty in identifying each blood fraction by conventional gating of blood cells using light scatter (FSC/SSC). As shown in Fig. 1, the guinea pig leukocytes were successfully gated into 4 leukocyte fractions using a novel gating method with MIL4/SSC in the blood and lymphoid tissues of the 60 young guinea pigs at the age of 8 weeks old.

As summarized in Table 3, the lymphocyte fraction was the major fraction at a level of 95% of tissue cells in both the lymph node (LN) and the thymus. The predominance of lymphocyte fraction was less in the spleen and the blood, at 68.2 ± 7.2 and 48.7 ± 14.1%, respectively. This lymphocyte fraction dominance in the

Table 3. Mean percentage of leukocyte fraction in the blood sample and lymphoid tissues of normal guinea pigs by novel flow cytometry using the MIL4/SSC parameter[a)]

		Mean	SD
Blood	Lymphocyte	48.7	14.1
	Monocyte	4.7	2.6
	Granulocyte	33.6	14.2
	KC	11.7	6.5
Spleen	Lymphocyte	68.2	7.2
	Monocyte	4.4	1.6
	Granulocyte	3.1	1.4
	KC	19.4	7.3
Thymus	Lymphocyte	96.5	0.6
	Monocyte	0.6	0.2
	Granulocyte	0.1	0.0
	KC	2.5	0.8
LN	Lymphocyte	94.8	1.4
	Monocyte	1.1	0.4
	Granulocyte	0.1	0.1
	KC	1.8	0.4

[a)] Leukocytes of guinea pigs were gated into 4 fractions by flow cytometry using the MIL4/SSC parameter shown in Fig. 1A. Data are expressed as the mean ± SD. N=60.